

Capture reactions with protons, neutrons, and alpha particles

H. R. Weller and N. R. Roberson

Duke University and Triangle Universities Nuclear Laboratory, Durham, North Carolina 27706

A review of recent capture experiments which discusses polarized proton, polarized neutron, and alpha particle capture reactions is presented. The giant dipole resonance region is examined chiefly in terms of the information which can be obtained from angular distribution measurements. Experimental results regarding the relative transition matrix elements and their phases are shown to be quite well accounted for by the direct-semidirect reaction theory. Some of the new information obtained from such experiments in the case of the three and four-body problems is described. The utility of polarized capture for the study of M1 and E2 strength is exhibited by examples. Several cases are shown in which the E2 strength observed in light nuclei via p capture is accounted for by a purely direct E2 mechanism. The virtues of polarized neutron capture studies are explored, and the results of the first experiments are described. Alpha particle capture is compared with p and n capture. Fundamental differences in the reaction processes are described which can account for the relatively small a_1 coefficients observed in n versus p capture and lack of E1-E2 coherence observed in several α -capture experiments.

CONTENTS

I. Introduction	699
A. Proton and neutron capture	699
B. Alpha capture	701
II. Angular Distribution Formalism for Particle Capture-Gamma Reactions	701
A. Channel spin representation	701
B. j - j coupling representation	702
III. Experimental Techniques	703
IV. Experimental Results	704
A. The giant dipole resonance and polarized proton capture	704
B. Polarized proton capture and M1 and E2 strength	708
C. Polarized proton capture involving few nucleon systems	713
1. The ${}^3\text{H}(p, \gamma){}^4\text{He}$ reaction	713
2. The ${}^2\text{H}(p, \gamma){}^3\text{He}$ reaction	714
D. E2 strength and polarized neutron capture	715
E. Alpha capture and E2 strength	720
V. Conclusions	721
Acknowledgments	722
Appendix: E2 Energy-Weighted Sum Rules	723
References	724

I. INTRODUCTION

The giant dipole resonance (GDR) in nuclei has been a subject of interest for many years. Radiative capture reactions have been extensively employed as a means of studying the detailed structure of the GDR. The good energy resolution of tandem Van de Graaffs has made such studies especially fruitful. Since a capture reaction only measures the decay of the GDR through one channel, the most intensively studied nuclei have been the light nuclei, where one channel often carries a significant fraction of the classical dipole sum rule. Of course the larger energy spacing between states in the residual nuclei favors these studies from the experimental side.

The discovery of the compact isoscalar giant quadrupole resonance (GQR) (Pitthan and Walcher, 1971; Fukuda and Torizuka, 1972; Lewis and Bertrand, 1972; Bertrand, 1976) has been largely responsible for a recent increase in the number of experiments using

the capture reaction. This interest has been further stimulated by two technical advances. The first is the availability of large NaI detector assemblies having an energy resolution of $\sim 3\%$ for ~ 20 MeV γ rays. The second is the availability of reasonably intense beams of polarized particles. These developments have led to new experimental studies of the GDR region using polarized proton, polarized neutron, and alpha particle capture reactions. These studies have been aimed at increasing our knowledge of both the GDR and the GQR, as well as the capture reaction process itself. Several reviews of some aspects of these studies have been previously written (Hanna, 1972, 1974, 1977, 1979; Glavish, 1973, 1976; Paul, 1977; Snover, 1979).

This paper will concern itself with a discussion of the results of three types of capture experiments: (p, γ) , (n, γ) , and (α, γ) . Both polarized and unpolarized projectiles will be considered when appropriate. We shall discuss the energy region which contains the giant dipole resonance ($E_x \sim 80/A^{1/3}$ MeV) (Hayward, 1970) and presumably the giant isoscalar quadrupole resonance ($E_x \sim 63/A^{1/3}$ MeV) [e.g., Moss *et al.* (1974); Youngblood *et al.* (1976)]. In particular, we shall concern ourselves with the information which can be obtained from angular distribution measurements. We begin by giving a brief discussion of what is thought to be an appropriate model for each of the three capture reactions to be considered.

A. Proton and neutron capture

It has been shown that proton capture excites the giant dipole resonance (GDR) predominantly through direct or semidirect processes. (Brown, 1964; Singh *et al.*, 1965; Snover *et al.*, 1976; Dietrich *et al.*, 1977). Indeed, the most widely used reaction model for fast-nucleon capture is the so-called direct-semidirect model (Brown, 1964; Clement *et al.*, 1965; Lushnikov and Zaretsky, 1965). In this picture the transition amplitude is expressed as the sum of two terms, one of which is called the direct term and represents the situation in which the incoming nucleon undergoes a radiative transition from its scattering

state into a single-particle bound state of the residual nucleus (Rolfs, 1973). The other term represents the semidirect or collective process. In this latter case the incoming nucleon inelastically excites the target nucleus into a collective state while occupying the *same* single-particle bound state as in the direct process. The subsequent radiative de-excitation of the excited target nucleus produces the enhanced gamma ray transition strength associated with the giant resonance.

An example of the behavior of the two separate cross sections (direct and semidirect) can be seen in Clement *et al.* (1965) and Cvelbar and Whetstone (1972). The simple direct-capture mechanism has been discussed in detail by Rolfs (1973, 1974). This smoothly varying cross section, characteristically of the order of 1 to 10 μb for proton capture, arises from the overlap of the single particle strength in the channel wavefunction with the state formed by the dipole operator acting on the ground state. It typically accounts for about 10% of the cross section in the region of the GDR. In the context of the schematic model (Brown, 1967) this strength is related to the particle-hole strength which does not get "pushed up" by the residual interactions. Direct capture is expected to dominate at energies below and above the giant resonance region and should be a useful tool for extracting spectroscopic information about the final states (Rolfs, 1973). At low energies contributions from compound nucleus states can complicate this picture.

The two-step semidirect capture amplitude takes account of most of the sum rule since it represents the excitation of the collective giant resonance state [e.g., Cvelbar and Whetstone (1974)]. Of course only a small fraction of this sum rule will, in general, be observed in the capture channel. According to Brown (1964) the direct and semidirect (collective) capture amplitudes are coherent, with the interference being destructive below and constructive above the peak energy.

In the direct-semidirect (DSD) theory the radial part of the transition amplitude is usually calculated according to [e.g., Potokar *et al.* (1977); Likar *et al.* (1976)]

$$\langle u_b | d^L | \chi^{(+)} \rangle + \langle u_b | h^L(r) | \chi^{(+)} \rangle / E - E_R + i\Gamma/2. \quad (1)$$

In this expression u_b is the radial wave function of the captured nucleon in the bound state, while $\chi^{(+)}$ is the continuum state calculated from the optical model potential. The quantity d^L represents the radial part of the single-particle electromagnetic operator for radiation of multipolarity L ; E_R and Γ refer to the position and width of the appropriate giant resonance of the combined target-plus-nucleon system, respectively, while $h^L(r)$ represents the radial part of the incident nucleon-target nucleus vibration coupling interaction (i.e., the form factor responsible for the inelastic excitation of the collective state by the incident nucleon). In this model the effect of the coupling between the incident particle and the giant resonance states is treated as a perturbation induced by the interaction Hamiltonian between the incident nucleon and the nucleons in the target nucleus. Various authors have suggested different expressions for this form factor (Brown, 1964; Clement *et al.*, 1965; Potokar, 1973). However, the

angular distributions do not appear to be extremely sensitive to the choice of form factor (Likar *et al.*, 1977). It will be seen, in fact, that the Brown form factor [$h^L(r)\alpha r$] (Brown, 1964) provides a reasonable description of the angular distributions observed in many p and n capture experiments.

An important point for our purposes is the fact that, when computing the cross section, the first term in the above expression, the so-called direct-capture term, is multiplied by a scaling factor which is the recoil effective charge (Hayward, 1970). This factor can be written for electric multipoles of order L as (Buck and Pilt, 1977)

$$\epsilon_L = (A_2^L Z_1 + (-)^L Z_2 A_1^L) / (A_1 + A_2)^L \quad (2)$$

where 1 and 2 refer to the projectile and the target, respectively. For $E1$ radiation we see that for protons $\epsilon = N_2 / (1 + A_2)$, while for neutrons $\epsilon = -Z_2 / (1 + A_2)$. In the case of E_2 radiation $\epsilon = (A_2^2 + Z_2) / (1 + A_2)^2$ for protons, and $\epsilon = Z_2 / (1 + A_2)^2$ for neutrons. Therefore, direct $E2$ radiation will be significantly reduced in the case of neutron capture relative to proton capture. This direct $E2$ radiation will be coherent with respect to the dominant $E1$ radiation and will vary smoothly with energy, reflecting the broad single-particle resonances of the optical potential, as well as the momentum matching of the bound and continuum wave functions. Since a significant amount of this *direct* $E2$ strength will normally be present in proton capture, it must be separated out before one can relate any observed $E2$ strength to collective radiation. In the case of neutron capture, however, the small recoil effective charge for quadrupole radiation means that direct $E2$ capture is essentially negligible (Arthur *et al.*, 1974). Therefore, within this model, any $E2$ radiation observed in a neutron capture reaction can be attributed to semidirect processes. Furthermore, as will be discussed in Sec. IV.D, since this $E2$ strength is observed by virtue of its interference with $E1$ amplitudes, the possibility of significant statistical compound nucleus contributions can be ruled out, provided that the compound nucleus levels are sufficiently broad and overlapping so that a complete averaging of any interference terms occurs.

The recent work of Dietrich and Kerman (1979) has introduced the pure-resonance model (PRM) for radiative capture, which has shed new light on some aspects of the DSD model. Their work is based on the Feshbach reaction formalism (Feshbach, 1962) and projects the GDR, described using a schematic model, out of the continuum space. These authors originally derived the DSD theory (as well as their PRM theory) under the assumption that the entire $E1$ strength of the system is in the GDR. This leads to the result that their formal semidirect amplitude contains a term which subtracts the direct amplitude. They point out that when different phenomenological ingredients are used in the two amplitudes in actual DSD calculations, this exact cancellation may be lost. Further investigations (Dietrich, 1979) have shown that the "pygmy" resonance strength (the dipole strength not pushed up by the residual interactions) needs to be included in the PRM, especially for light nuclei. When this is done, it has been found that the two models (DSD and PRM) can

be made to be equivalent (Kerman, 1980). It now appears as though the PRM model represents a formulation of the capture problem which, in some cases, may provide a calculational technique which is less sensitive to certain parameters which appear in the DSD model.

This paper will not deal with the detailed predictions of the DSD or the PRM models for cross sections as a function of energy. However, we shall demonstrate that the DSD model can successfully describe the main features of the angular distributions observed in capture reactions. It will also be seen that a pure direct-capture calculation (no collective enhancement) can account for the $E2$ strength observed in several (p, γ) capture experiments—indicating that the $E2$ giant resonance is not important in the capture channel in these cases.

B. Alpha capture

The alpha capture reaction employing a spin zero target nucleus is an attractive means for searching for $E2$ resonance strength. In this case, if we assume only $E1$ and $E2$ contributions, the angular distribution can be written as [e.g., Meyer-Schützmeister *et al.* (1978)]

$$\sigma(\theta) = A \sin^2\theta + B \sin^2 2\theta + C \sin\theta \sin 2\theta, \quad (3)$$

where

$$\sigma(E1) = 8\pi A/3; \quad \sigma(E2) = 32\pi B/15; \quad \cos\theta_{12} = C/2(AB)^{1/2}, \quad (4)$$

θ_{12} denoting the phase angle between the $E1$ and the $E2$ amplitude. The experimental angular distributions, when fitted to the above expression, often indicate that $\langle \cos\theta_{12} \rangle \sim 0$ ($\theta_{12} \sim 90^\circ$). This suggests the possibility that the two amplitudes are adding incoherently. Since several analyses have shown that α capture into the GDR is predominantly a statistical process (Meyer-Schützmeister *et al.*, 1968; Foote *et al.*, 1976), it seems reasonable to conclude that this is the reason for the lack of coherence between the $E1$ and $E2$ amplitudes. That is, the $E1$ strength results from a great number of overlapping resonances which give rise to so many interference terms with respect to any $E2$ amplitudes that the average is close to zero—at least when the experimental energy spread is large compared to the width of the individual resonances. Indeed, the deviations from $\theta_{12} = 90^\circ$ are observed to diminish as the structure in the yield curve disappears with increasing A [e.g., Meyer-Schützmeister *et al.*, 1978; Kuhlmann *et al.* (1979)]. Since the statistical nature of the $E1$ strength destroys any possible interference with respect to any $E2$ strength which might be present, the angular distribution data cannot be used to tell us whether the $E2$ amplitude is itself statistical or not. We will see, however, that the magnitude of the $E2$ strength observed in several (α, γ) reactions suggests that there is a nonstatistical component present in the (α, γ) reaction which proceeds through the GQR. (Meyer-Schützmeister *et al.*, 1978; Kuhlmann *et al.*, 1975, 1979).

II. ANGULAR DISTRIBUTION FORMALISM FOR PARTICLE CAPTURE-GAMMA REACTIONS

One of this paper's primary interests is to review the information obtained from angular distribution measurements of radiation resulting from the capture of neutrons, protons, and alpha particles in the giant resonance region. In the case of neutrons and protons we are considering the situation in which beams of po -polarized particles are also employed. In order to extract information from the measured angular distributions, a reaction formalism must be utilized. Although the necessary expressions have been previously published (Devons and Goldfarb, 1957; Baldin *et al.*, 1961; Welton, 1963; Laszewski and Holt, 1977), recent work has shown that the literature expressions contain some errors (Seyler and Weller, 1979). A brief summary of this situation is therefore presented below.

Suppose we consider an x capture- γ reaction whose angular momenta are specified by

$$a(x, L)c, \quad (5)$$

where a is the spin of the target, x is the spin of the projectile carrying angular momentum l , b is the spin of the γ -emitting (intermediate) state, L is the multipolarity, and p the mode (1 electric, 0 magnetic) of the gamma ray, and c is the spin of the residual state after the gamma emission.

Now with $\hat{x} = (2x+1)^{1/2}$, we define a set of Legendre polynomial coefficients by the equation

$$\sigma(\theta) = \left(\frac{1}{2}\lambda\right)^2 \hat{x}^{-2} \hat{a}^{-2} \sum_{k=0}^n Q_k \bar{a}_k P_k(\cos\theta). \quad (6)$$

An alternative form of this equation is

$$\sigma(\theta) = A_0 \left[1 + \sum_{k=1}^n Q_k a_k P_k(\cos\theta) \right], \quad (7)$$

where $a_k = \bar{a}_k/\bar{a}_0$, and $A_0 = \left(\frac{1}{2}\lambda\right)^2 \hat{x}^{-2} \hat{a}^{-2} \bar{a}_0$. Equation (7) is the expression normally used in fitting experimental data. The coefficients Q_k are the usual angular attenuation coefficients which correct for the finite geometry of the experimental setup (Ferguson, 1965).

When polarized proton or neutron beams are employed, the analyzing power

$$A(\theta) = \frac{1}{P} \frac{N_+ - N_-}{N_+ + N_-} \quad (8)$$

can be measured. In this expression N_+ and N_- are the yields obtained for spin-up and spin-down beams (in the Madison convention), respectively, and P is the beam polarization. The analyzing power data are expanded according to

$$\frac{\sigma(\theta)A(\theta)}{A_0} = \sum_{k=1}^n Q_k b_k P_k^1(\cos\theta). \quad (9)$$

A. Channel spin representation

The a_k and b_k coefficients obtained from these expansions of the experimental data can now be related to the reduced transition matrix elements. The first step necessary in order to obtain these relationships is to choose a coupling scheme and then to choose a coupling order. For example, we may choose to use

the channel spin representation and adopt the coupling order:

$$\begin{aligned} \mathbf{x} + \mathbf{a} &= \mathbf{s}, \\ \mathbf{l} + \mathbf{s} &= \mathbf{b}, \\ \mathbf{L} + \mathbf{c} &= \mathbf{b}. \end{aligned}$$

We now denote the reduced transition matrix elements as

$$T \equiv \langle pL(c)b\pi \| T \| l(xa)sb\pi \rangle$$

and

$$T' \equiv \langle p'L'(c)b'\pi' \| T \| l'(xa)s'b'\pi' \rangle. \quad (10)$$

Expressions for the Legendre coefficients can now be derived in terms of these (complex) matrix elements. The expressions for the Legendre coefficients in terms of the transition matrix elements in LS coupling are

$$A_0 = \left(\frac{1}{2}\lambda\right)^2 \hat{x}^{-2} \hat{a}^{-2} \sum_t \hat{\delta}^2 |T|^2, \quad (11)$$

$$a_k = \frac{\left(\frac{1}{2}\lambda\right)^2 \hat{x}^{-2} \hat{a}^{-2}}{A_0} \left\{ \sum_{tt'} (-)^{s-c+1} [\hat{l} \hat{l}' \hat{L} \hat{L}' \hat{b}^2 \hat{b}'^2 (l0, l'0 | k0) \right. \\ \left. \times W(lb l' b'; sk) (L1, L' - 1 | k0) \right. \\ \left. \times W(Lb L' b'; ck) \operatorname{Re}(TT'^*) \right\}, \quad (12)$$

and

$$b_k = \frac{\left(\frac{1}{2}\lambda\right)^2 \hat{x}^{-2} \hat{a}^{-2}}{A_0} \\ \times \left\{ \frac{3\sqrt{x} \hat{x} \hat{k}}{[(x+1)k(k+1)]^{1/2}} \sum_{tt'} [\hat{s} \hat{s}' \hat{l} \hat{l}' \hat{L} \hat{L}' \hat{b}^2 \hat{b}'^2 \right. \\ \left. \times (-1)^{a-x+c-b-s+l} (l0, l'0 | k0) \right. \\ \left. \times W(xsx s'; a1) (L1, L' - 1 | k0) \right. \\ \left. \times W(Lb L' b'; ck) \right. \\ \left. \times X(lsb; l' s' b'; k1k) \operatorname{Re}(iT T'^*) \right\}. \quad (13)$$

The sum over l and l' means over $pp'LL'bb'W$'s and s' . The empty bracket is defined to be

$$[] \equiv \frac{1}{2} [1 + (-)^{L+p+L'+p'+k}]. \quad (14)$$

Tables which permit one to evaluate these relations exist in the literature (Carr and Baglin, 1971; Laszewski and Holt, 1977). However, as has been pointed out (Seyler and Weller, 1979), the tables for the b_k coefficients, based on the results of Baldin *et al.* (1961), must be corrected by an additional phase factor:

$$(-1)^{(L+J+S)_{\text{first}} - (L+J+S)_{\text{second}} + 1}. \quad (15)$$

In obtaining this expression the connection between $P_\nu^1(x)$ and $\bar{P}_\nu^1(x)$ was taken as defined in Baldin *et al.* (1961):

$$\bar{P}_\nu^1(x) = - \left(\frac{2\nu+1}{2\nu(\nu+1)} \right)^{1/2} P_\nu^1(x). \quad (16)$$

B. j - j coupling representation

In j - j coupling we can couple as follows:

$$\begin{aligned} \mathbf{l} + \mathbf{s} &= \mathbf{j}, \\ \mathbf{j} + \mathbf{a} &= \mathbf{b}. \end{aligned}$$

The results in this scheme are:

$$A_0 = \left(\frac{1}{2}\lambda\right)^2 (\hat{x}^{-2} \hat{a}^{-2}) \sum_t \hat{\delta}^2 |T|^2, \quad (17)$$

$$a_k = \frac{\left(\frac{1}{2}\lambda\right)^2 (\hat{x}^{-2} \hat{a}^{-2})}{A_0} \\ \times \left\{ \sum_{tt'} (-)^{a-c+1-x+k+j-j'} \hat{j} \hat{j}' \hat{l} \hat{l}' \hat{L} \hat{L}' \hat{b}^2 \hat{b}'^2 (l0, l'0 | k0) \right. \\ \left. \times W(lj l' j'; xk) \right. \\ \left. \times [] (L1, L' - 1 | k0) W(jb j' b'; ak) \right. \\ \left. \times W(Lb L' b'; ck) \operatorname{Re}(TT'^*) \right\}, \quad (18)$$

and

$$b_k = \frac{\left(\frac{1}{2}\lambda\right)^2 (\hat{x}^{-2} \hat{a}^{-2})}{A_0} \left\{ \frac{3\sqrt{x} \hat{x} \hat{k}}{[(x+1)k(k+1)]^{1/2}} \right. \\ \left. \times \sum_{tt'} \hat{j} \hat{j}' \hat{l} \hat{l}' \hat{L} \hat{L}' \hat{b}^2 \hat{b}'^2 (-)^{a-c+1+l'-j'} [] \right. \\ \left. \times (l0, l'0 | k0) W(jb j' b'; ak) (L1, L' - 1 | k0) \right. \\ \left. \times W(Lb L' b'; ck) X(lxj; l'xj'; k1k) \operatorname{Re}(iT T'^*) \right\}. \quad (19)$$

Other expressions which exist in the literature also allow for the evaluation of the b_k coefficients in terms of the transition matrix elements. For example, the work of Welton (1963) can be used. However, it has also been observed that for the present case of polarized projectiles incident on unpolarized targets the expression of Welton is in error by a factor of $(-)^6$ (Seyler and Weller, 1979).

In the case of j - j coupling the b_k expressions can be obtained from the a_k expressions by use of a relatively simple relationship (Devons and Goldfarb, 1957). If we have

$$a_k = \sum_{tt'} C_{tt'} \operatorname{Re}(T_t T_{t'}^*), \quad (20)$$

then

$$b_k = \frac{3/2}{x+1} \sum_{tt'} C_{tt'} f_k \operatorname{Re}(iT_t T_{t'}^*), \quad (21)$$

where

$$f_k = \frac{j(j+1) - l(l+1) - j'(j'+1) + l'(l'+1)}{k(k+1)}. \quad (22)$$

Given these expressions, the analysis of experimental data in terms of the transition matrix elements is rather straightforward. In general, two procedures have been used. In the first the data are used to obtain the a_k and b_k coefficients by performing a least-squares fit to the expansions given by Eqs. (7) and (9). These coefficients are then written in terms of the T -matrix elements and the resulting equations are solved by

varying the amplitudes and phases of the T -matrix elements to minimize chi-square. Alternatively, one can bypass the intermediate step of obtaining the a_k and b_k coefficients and fit the data by varying the amplitudes and phases to minimize chi-square directly. Of course, both procedures yield identical results, although some discrepancies in error estimates can arise if the proper weight matrix is not propagated in the two-step procedure (Bussoletti *et al.*, 1976). In obtaining these solutions it has been found necessary, because of the nonlinear nature of the least-squares fitting procedure, to examine carefully the chi-square function for multiple minima.

III. EXPERIMENTAL TECHNIQUES

Assuming the availability of the appropriate beams, the essential apparatus necessary for performing radiative capture measurements in the giant resonance region is the large NaI detector. A review of large NaI detectors has been previously published (Paul, 1974). Much of the data to be reported in this article were obtained with such a system at the Triangle Universities Nuclear Laboratory (TUNL) (Weller *et al.*, 1976). Some of the essential operating characteristics of this particular system will be described here.

A schematic diagram of the experimental setup at TUNL is shown in Fig. 1. The 25.4×25.4 cm NaI detector is viewed by six RCA 8575 photomultiplier tubes. The use of a collection of small tubes is now regarded as essential for achieving the best resolution from such a system. The NaI detector is surrounded by an NE-110 plastic annulus, which is viewed by eight XP-1031 photomultiplier tubes. This shield is run in anticoincidence with the NaI detector, as discussed by Paul (1974). Additional passive shielding, shown in Fig. 1, is necessary to reduce the count rates in both the NaI detector and the plastic shield. The present system uses 10 cm of lead, 20 cm of paraffin doped with Li_2CO_3 (about 50% by weight), and 0.16 cm thick cadmium sheet for this purpose.

The resolution and the gain of this system are count rate dependent. In the present case it has been found that if the total NaI count rate is kept below 2×10^5 cts/

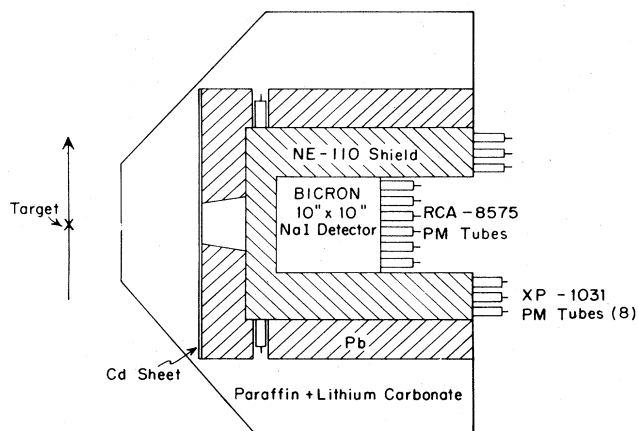


FIG. 1. Schematic diagram of the NaI(Tl) spectrometer system at TUNL.

sec, then the gain does not show any apparent variations and a resolution of about 3% at $E_\gamma = 20$ MeV can be achieved. With the shielding arrangement in the TUNL system, the typical NaI count rate is $\sim 10^5$ cts/sec. Due to the high count rate experienced by the NaI detector, fast electronics are necessary to reduce the probability of pulse pileup (Paul, 1974). The technique used in the TUNL system consists of clipping the direct anode signal by using a $50\text{-}\Omega$ cable terminated with a resistor chosen to obtain the best base-line restoration. This signal is sent through a fast linear gate (~ 300 to 400 nsec width), which is opened only if the clipped pulse (~ 20 nsec) generating the gate is large enough to generate an enabling pulse. This procedure eliminates the pileup of two "small" pulses which occur in a time interval greater than ~ 20 nsec. After the gate is opened for 400 nsec, it is held closed for the signal processing time (~ 10 μ sec).

The efficiency of this detector system has been determined by employing the $^{12}\text{C}(p, \gamma_0)$ reaction, since an accurate measurement of the number of γ rays per proton has been reported for the 15.07 MeV resonance in ^{13}N (Marrs *et al.*, 1975). A "thick" (~ 50 keV for 14.2 MeV protons) ^{12}C target was employed to obtain the integrated resonance yield. The response function was summed using a standard line shape obtained from the $T(p, \gamma)^4\text{He}$ reaction. This line shape was subsequently employed in summing other measured yields. The results of this calibration yielded an efficiency of 0.17 ± 0.012 for the present system. This number was checked by considering the various factors which contribute to the efficiency. The fraction of the total response which appeared in the peak region was obtained from a spectrum obtained by Hayward *et al.* (1979), using monochromatic 15.1 MeV γ rays and a 25.4×25.4 cm NaI crystal. This number was corrected for the rejection due to the plastic anticoincidence shield in our experiment and the attenuation effects of the shielding material placed in front of our detector. The result of this analysis was an overall efficiency which agreed within error with the quoted result.

In order to obtain the efficiency of the detector system at other energies, several energy-dependent effects must be measured and taken into account. A preliminary measurement of the energy dependence of the NaI detector response function has been obtained by Hayward *et al.* (1979). In addition, the energy dependence of the attenuation due to the shielding in front of the detector as well as the energy dependence of the rejection efficiency of the anticoincidence shield can be measured.

The experimental setup used for most of the fast neutron capture studies to be discussed in this article is shown in Fig. 2. The neutron source used here was the $^2\text{H}(d, n)^3\text{He}$ reaction with a pulsed (sometimes polarized—see below) beam incident on a gas cell. The deuterium gas cell was 3.0 cm long and was pressurized to 3.0 atm. The entrance foil for this cell was a 4.6 μm thick molybdenum foil. The tungsten shadow bar, shown in Fig. 2, was the essential change in shielding made in the system with respect to the configuration used for proton capture studies. The pulsed beam is used to generate a time of flight signal. An

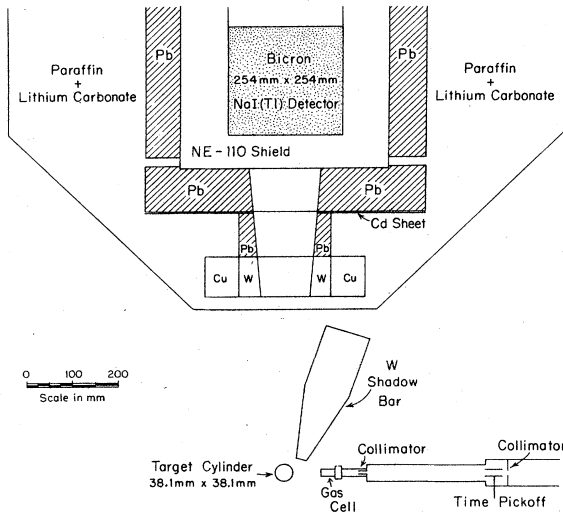


FIG. 2. Experimental arrangement used at TUNL for neutron capture studies. The neutron production facility which employs the ${}^2\text{H}(d, n){}^3\text{He}$ reaction is indicated.

overall time resolution of 3.5 nsec provided effective discrimination against neutron-induced background. It has been found that in studying reactions with Q values ~ 7 MeV this discrimination becomes important only for neutron energies less than 7 MeV and for angles less than $\sim 50^\circ$. A spectrum which illustrates the performance of this system and the resolution of our NaI detector is shown in Fig. 3 for the case of ${}^{40}\text{Ca}(n, \gamma){}^{41}\text{Ca}$; several others have been presented in the literature [e.g., Weller *et al.* (1976); Cameron *et al.* (1976); Turner *et al.* (1978)] in the case of proton capture.

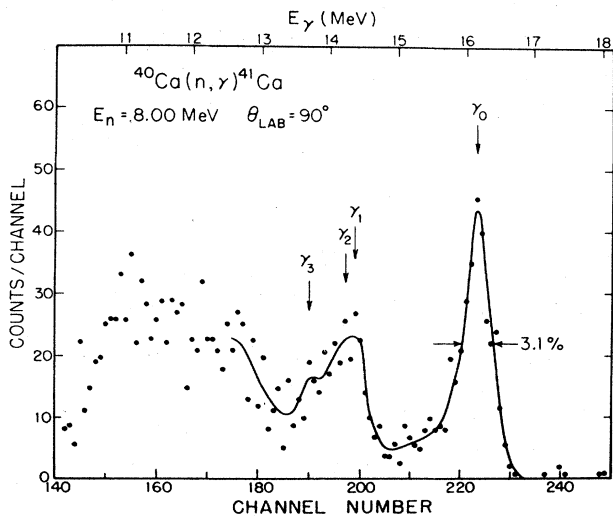


FIG. 3. Spectrum obtained for the ${}^{40}\text{Ca}(n, \gamma){}^{41}\text{Ca}$ reaction using the spectrometer system shown in Fig. 2. The pulsed beam was used in obtaining this spectrum. An overall time resolution of 3.5 nsec provided effective discrimination against neutron induced background. The solid curve is a smooth curve drawn through the data points.

IV. EXPERIMENTAL RESULTS

A. The giant dipole resonance and polarized proton capture

The results of polarized proton capture measurements in the region of the GDR have been interpreted in terms of the direct-semidirect (DSD) model (Shover, 1974, 1979) and the doorway-state model (Feshbach *et al.*, 1967; Mavis, 1977). In our presentation of these studies we shall first consider only the giant dipole ($E1$) resonance and the DSD model. In the next section we shall consider the extension of the measurements and the calculations to the case when the effects of $E2$ radiation are included.

The first report of a polarized proton capture study in the giant dipole resonance region was for the case of ${}^{11}\text{B}(p, \gamma){}^{12}\text{C}$ (Glavish *et al.*, 1972). These results demonstrated that rather large analyzing powers could be observed, thus indicating coherence between the various T -matrix elements involved in the reaction. This work was followed by a study of ${}^{16}\text{O}$ via the ${}^{15}\text{N}(p, \gamma){}^{16}\text{O}$ reaction (Hanna *et al.*, 1972). Again the asymmetry was observed to be large and "remarkably constant" over the structure of the giant resonance. An analysis was performed to determine the two contributing $E1$ matrix elements. Writing the complex matrix elements in terms of a real amplitude and a phase, we can denote the $E1$ terms by the incoming partial waves in j - j coupling as $s_{1/2} \exp(i\phi_s)$ and $d_{3/2} \exp(i\phi_d)$. Then, neglecting all radiations except $E1$, we can write (see Sec. II.B)

$$\begin{aligned} 1.0 &= s_{1/2}^2 + d_{3/2}^2 \quad (\text{normalization}), \\ a_2 &= -0.5d_{3/2}^2 + 1.414s_{1/2}d_{3/2} \cos(\phi_s - \phi_d), \\ b_2 &= -0.707s_{1/2}d_{3/2} \sin(\phi_s - \phi_d). \end{aligned} \quad (23)$$

The solutions shown in Fig. 4 are from Bussoletti (1978), and represent recent results obtained from an analysis which allowed for $E2$ amplitudes in addition to the $E1$ amplitudes discussed above. The $E2$ terms do not have a significant effect on the $E1$ terms in this case. The point here is to notice that there are two solutions. Solution I (solid circles) is characterized by dominant $d_{3/2}$ capture while solution II (x 's) corresponds to mainly $s_{1/2}$ capture. The remarkable feature of these results is the constancy of the relative $s_{1/2}$ and $d_{3/2}$ amplitudes across the entire region of the GDR. Similar studies of the $E1$ amplitudes and phases in the giant dipole resonance region were subsequently performed on a number of target nuclei (Weller *et al.*, 1976, 1978; Turner *et al.*, 1978, 1979; Cameron *et al.*, 1976). The results for targets of ${}^{13,14}\text{C}$, ${}^{30}\text{Si}$, ${}^{88}\text{Sr}$, ${}^{54,56,58}\text{Fe}$, and ${}^{59}\text{Co}$ are shown below in Fig. 5. The procedure used to obtain the data points shown here was the same as in Hanna (1972). Namely, measured values of $\sigma(\theta)$ and $A(\theta)$ were used to obtain A_0 , a_2 , and b_2 , which were then, assuming pure $E1$ radiation, written in terms of the contributing $E1$ T -matrix elements. It is important to note here that in the last four cases all the final nuclei have $7/2^-$ ground-state spins. This means that there are three T -matrix elements which can contribute to the $E1$ strength: $d_{5/2} \exp(i\phi_{d_{5/2}})$, $g_{9/2} \exp(i\phi_{g_{9/2}})$, and $g_{7/2} \exp(i\phi_{g_{7/2}})$. Having to determine three amplitudes and two relative phases means there are more unknowns

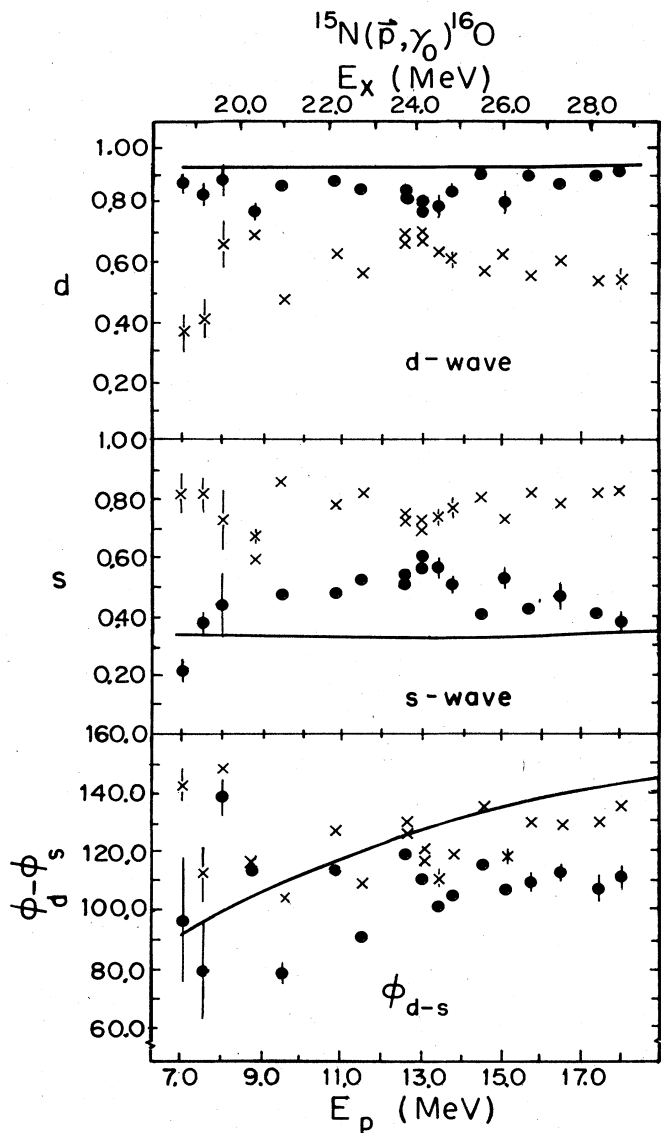


FIG. 4. The relative E1 capture amplitudes and their phase difference for the $^{15}\text{N}(p, \gamma)^{16}\text{O}$ reaction (Bussoletti, 1978). These solutions were obtained from an analysis which included both E1 and E2 amplitudes. Both dominant d-wave solutions (dots) and dominant s-wave solutions (crosses) are shown for the minimum E2 strength solution obtained by fitting all measurements at each energy. The solid curves are a result of the DSD calculation (described in the text) which used $h^1(r)\alpha r$.

than knowns, so that some simplifying assumption must be made to extract the T -matrix element information. Since the final single particle state in these cases is $f_{7/2}$, the $g_{7/2}$ T -matrix element should be small, since, if it goes as a single particle transition, it would be a spin-flip-like transition and hence negligible. Detailed calculations using the extended DSD theory (Potokar, 1978) and the continuum shell model (Halder-son, 1978) support the neglect of this term. The data of Fig. 5 were obtained by neglecting the $g_{7/2}$ term for the Fe and Co targets.

The analysis of the capture data described above has

the property of producing two solutions as a result of the quadratic nature of the equations for A_0 , a_2 , and b_2 . We shall now attempt to show that a model calculation, the DSD model in its simplest form, appears to be capable of selecting one of the two solutions as the correct or physical solution.

In the direct-semidirect (DSD) reaction model (Cvelbar and Whetstone, 1974; Snover *et al.*, 1976; Potokar, 1973) the computation of the T -matrix elements for the capture reaction requires the evaluation of a radial matrix element having the form given by Eq. (1) in Sec. I.A. Using the Brown form factor $[h^1(r)\alpha r]$ indicates that the semidirect cross section can be treated as a product of the direct capture cross section and a resonancelike factor (Cvelbar and Whetstone, 1974). So, provided that the resonance parameters are taken to be independent of the relevant angular momentum quantum numbers, a calculation of the relative amplitudes and phases obtained from a pure direct-capture model can be regarded as a DSD calculation with $h^1(r)\alpha r$.

The direct-capture cross section on spin-zero targets for electric radiation of multipolarity L is given in the long-wavelength limit by the expression:

$$\sigma_T^L = 4\pi\epsilon_L^2 \left(\frac{197.3289}{137.036} \right) \frac{k_f}{E_a k_a} \frac{(2j+1)}{(2x+1)} B_L^2 \sum_{l_a j_a} |T_{l_j; l_a j_a}^L|^2, \quad (24)$$

where

$$B_L^2 = \frac{L+1}{(2L+1)L} \frac{k_f^{2L}}{[(2L-1)!!]^2}, \quad (25)$$

and

$$T_{l_j; l_a j_a}^L = i^{l_a - l - L} C(j L j_a, \frac{1}{2} 0 \frac{1}{2}) \sqrt{C^2 S_{l_j}} \langle u_{l_j} | r^L | \chi_{l_a j_a}^{(+)} \rangle. \quad (26)$$

Note that k_f and k_a are the outgoing and incident wave number, respectively, while E_a is the incident center of mass energy. The quantum numbers l, j refer to the final (bound) single particle state having a spectroscopic factor of $C^2 S_{l_j}$, while l_a, j_a refer to the incident nucleon. The percentage of the cross section due to a given T -matrix element was evaluated using the normalization condition:

$$\sum_{l_j; l_a j_a} |T_{l_j; l_a j_a}^L|^2 = 1. \quad (27)$$

Note that the factor $\hat{\delta}^2(\hat{j}_a^2)$ does not appear in the normalization condition of Eq. (27). This is a result of the particular coupling order used in the Clebsch-Gordan coefficient above. The continuum wave function $\chi_{l_a j_a}^{(+)}$ is calculated using the optical model potential. The bound-state single-particle wave function u_{l_j} is obtained by integrating the Schrödinger equation and adjusting the Woods-Saxon potential, which includes a spin-orbit term, to reproduce the known bound-state energy.

A straightforward generalization of the DSD theory to the case of targets with spin follows if it is assumed that the semidirect process depends only on the final-state parentage to the target ground state plus a single nucleon (Snover, 1978). In this case the T -matrix element for the case of a target with spin a can be written in terms of the spin 0 target T -matrix elements:

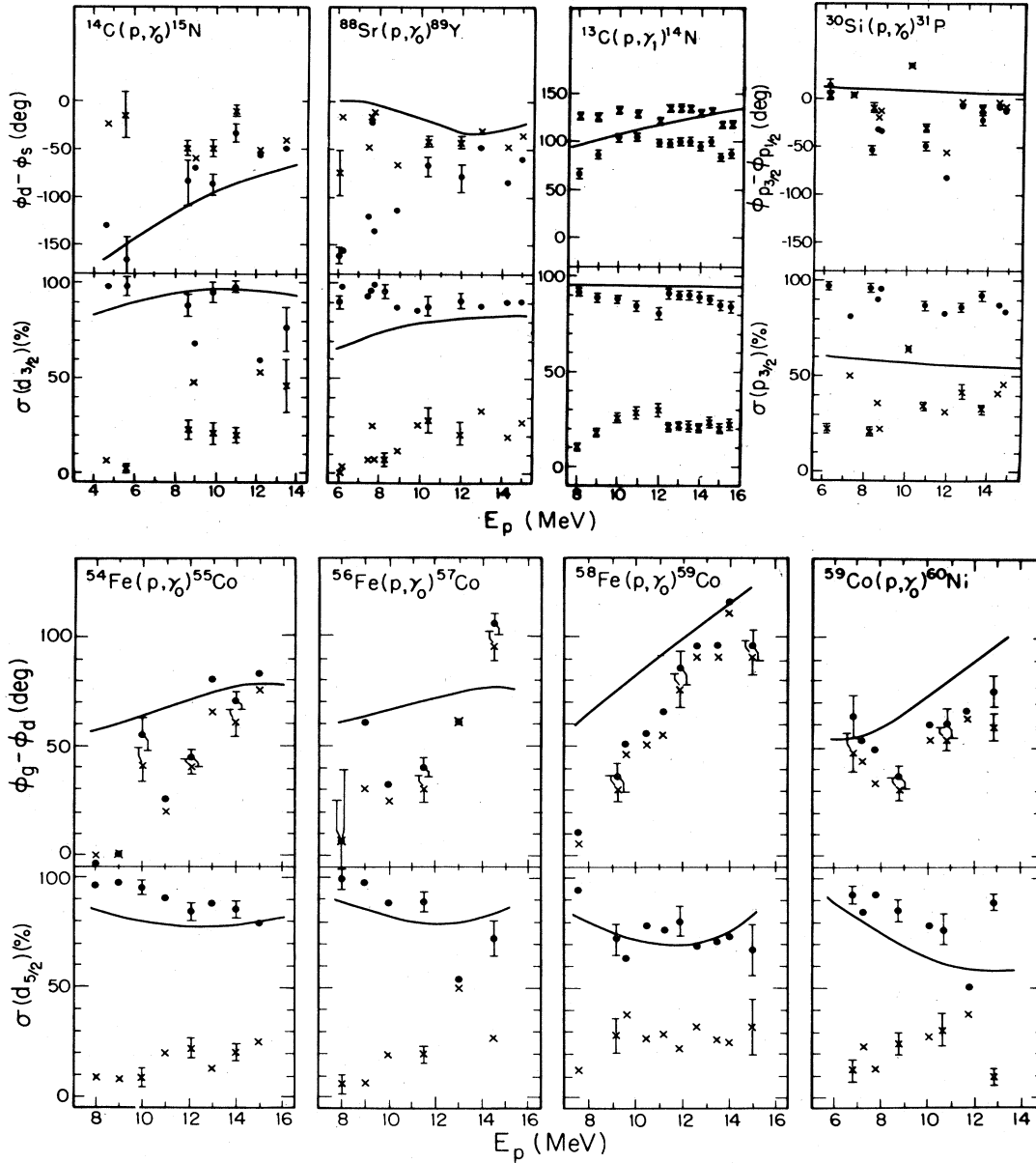


FIG. 5. The two solutions (dots and x 's) resulting from a pure $E1$ analysis of the cross section and analyzing power data are shown for target nuclei of ^{13}C , ^{14}C , ^{88}Sr , ^{30}Si , $^{54,56,58}\text{Fe}$, and ^{59}Co . The amplitudes are presented in terms of the percentage of the total $E1$ cross section for which they are responsible. The error bars represent (typical) statistical errors associated with the data points. The solid curves are the result of DSD calculations (described in the text) which $h^1(r)\alpha r$.

$$\langle Lcb \| T \| (lx)jab \rangle = \sum_{j''} \langle Lj''j \| T \| (lx)j0j \rangle \hat{c}j W(aj''bL; cj). \quad (28)$$

The quantity c is the spin of the final state which results from coupling the single-particle total angular momentum j'' to the target spin a . From this it follows that the equations to be used for the a_k and b_k coefficients when analyzing nonspin-zero target cases to obtain the spin-zero target T -matrix elements are essentially the spin-zero target equations where the final state has angular momentum j'' :

$$A_0 a_k = \sum_{j''} \frac{\hat{c}^2}{a^2 j''^2} \times \{ \text{spin-zero target expression with } j'' \text{ residual state} \}, \quad (29)$$

and

$$A_0 b_k = \sum_{j''} \frac{\hat{c}^2}{a^2 j''^2} \times \{ \text{spin-zero target expression with } j'' \text{ residual state} \}. \quad (30)$$

In addition, the cross section σ_T for the case with tar-

get spin a is related to the spin-zero target cross section by:

$$\sigma_T(\text{target spin } a) = \sum_{j''} \frac{\hat{c}^2}{\hat{a}^2 j''^2} \times \sigma_T(\text{target spin 0, residual } j''). \quad (31)$$

which follows from

$$A_0 = \sum_{j''} \frac{\hat{c}^2}{\hat{a}^2 j''^2} \times \{\text{spin-zero target expression with } j'' \text{ residual state}\}.$$

Note that if only one value of j'' is important in the final state, then the problem can be analyzed entirely as though it were a spin-zero target case except for the normalization factor on the absolute cross section.

The results of such calculations are shown as the solid curves in Figs. 4 and 5. Here it can be seen that if we concentrate on the results for the amplitudes, the calculation agrees much better with one of the two solutions obtained from the experiment with the exception of ^{30}Si (see below). Hence it appears that these relatively simple calculations provide a straightforward means for choosing the correct solution (Weller *et al.*, 1978). It should be noted that DSD calculations performed using more sophisticated form factors (real volume coupling) yield results in the cases of $^{15}\text{N}(p, \gamma)^{16}\text{O}$ and $^{14}\text{C}(p, \gamma)^{15}\text{N}$, which are essentially identical to those shown here (Snover, 1979).

The case of $^{30}\text{Si}(p, \gamma_0)^{31}\text{P}$ is clearly special in that the DSD calculation does not appear to favor either solution. This case differs from the others in that the two $E1$ amplitudes have the same l value and therefore a relatively small phase difference, which leads to a small b_2 coefficient. This apparently makes the $E1$ analysis very sensitive to the presence of non- $E1$ matrix elements, since, when an analysis is performed which includes the two possible $E2$ amplitudes, a solution is obtained for which the $p_{3/2}(E1)$ amplitude accounts for 60–70% of the $E1$ cross section. This solution is in agreement with the DSD calculation of Fig. 5 (Weller *et al.*, 1978). This case demonstrates that, under some circumstances, the neglect of non- $E1$ radiation can be serious.

Detailed studies of DSD calculations in the case of medium and heavy nuclei have revealed some difficulties (Snover, 1979). For example, an attempt has been made to establish the existence of an isovector GQR in ^{90}Zr (Dietrich *et al.*, 1977) by comparing the energy dependence of the measured a_k coefficients with the predictions of the DSD model. This effort is complicated by the sensitivity of the calculations to the rather uncertain strengths of the form factor. The effects of possible compound nucleus contributions, as well as the presence of isobaric analog resonances, further complicate this situation. However, as shown in Fig. 5 for the case of $^{88}\text{Sr}(p, \gamma_0)^{89}\text{Y}$, the DSD calculation with a form factor of r appears capable of selecting one of the two possible solutions for the relative amplitudes which contribute to the reaction at a given energy. This is especially true if the lower-energy region, where compound nucleus effects are expected to be more important, is ignored.

The heavy nuclei (e.g., ^{209}Bi) exhibit difficulties with regard to the DSD calculations, especially for capture to states of high angular momentum (Snover, 1979). However, $E1$ calculations using the pure resonance model (Dietrich and Kerman, 1979) appear to be able to account for the cross section data in the case of $^{209}\text{Pb}(n, \gamma)$ with a reduced sensitivity to the form factor parameters. Perhaps these calculations will prove to be more useful than the DSD calculations in this mass region, especially if one is trying to account for more than the angular distribution features of the problem.

In addition to providing insight into the dominant factors which determine the angular distributions observed in proton capture reactions, more detailed measurements with polarized proton capture reactions have provided new information on the nature of the intermediate structure observed in the giant dipole resonance of ^{16}O (Calarco *et al.*, 1977). In one such study measurements of the analyzing power were made on the reaction $^{15}\text{N}(p, \gamma_0)^{16}\text{O}$ in 100-keV steps between $E_x = 20$ and 24 MeV (Calarco *et al.*, 1977). The resulting b_2 coefficients were combined with A_0 and a_2 obtained from earlier work (O'Connell and Hanna, 1978; Hanna *et al.*, 1974), and used to extract the relative amplitudes and phases of the $E1$ T -matrix elements. The results of this analysis are shown in Fig. 6. The solid and open circles represent the two possible solutions.

These results indicate that the angular distribution coefficients display effects which are correlated with the intermediate structure of the GDR of ^{16}O . The present data were interpreted by introducing a narrow secondary doorway state which interferes with the primary GDR of ^{16}O . In this case the secondary doorway was assumed to be an α particle ($4p-4h$) state at 21.1 MeV, as observed in the $^{12}\text{C}(\alpha, \gamma)$ reaction (Suffert and Feldman, 1967; Snover *et al.*, 1974). Using the doorway state formalism of Feshbach, Kerman, and Lemmer (1967) and referring to the primary doorway by the subscript B and to the secondary doorway by the subscript A , one can write the T -matrix element for a given proton channel l, j as

$$T_{l,j} = \exp(i\phi_B^l) \frac{g_B^{l,j} g_B^\gamma (E - E_A + i\Gamma_A/2) + g_A^{l,j} |V| \exp(-i\mathfrak{K}^l) g_B^\gamma}{(E - E_B + i\Gamma_B/2)(E - E_A + i\Gamma_A/2) - |V|^2}, \quad (33)$$

where the quantities $g^{l,j}$ and g^γ are the square roots of the particle and γ -decay widths (Calarco *et al.*, 1977; Kabachnik and Rayuvaev, 1976). The phases ϕ_B^l and $\mathfrak{K}^l = \phi_B^l - \phi_A^l$ were treated as free parameters, the primary doorway energy E_B was fixed at 22.5 MeV, and it was assumed that resonance A has no intrinsic γ decay width. The observed energy and width of resonance A were used to constrain the energy, width, and interaction strength parameters E_A , Γ_A , and V .

The assumption of physical continuity allows the definition of two solutions as shown in Fig. 6. Solution I is dominant d -wave and is represented by the solid dots in Fig. 6. When the two resonance model is fitted to the lower s -wave solution (I), a χ^2 is obtained which is better by more than a factor of 2 than χ^2 for any alternative possibility. Hence it has been concluded (Calarco *et al.*, 1977) that if the two resonance model

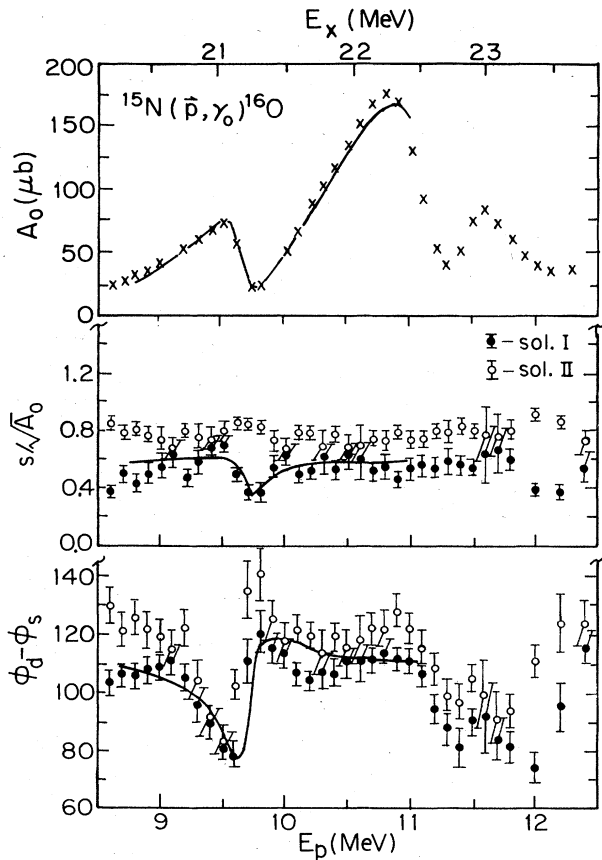


FIG. 6. The integrated cross section is shown (O'Connell and Hanna, 1978) along with the two solutions for the normalized s -wave amplitude and the relative phase obtained from the $^{15}\text{N}(p, \gamma)^{16}\text{O}$ data. The d strength is determined by the condition $(s^2 + d^2)/A_0 = 1$. The solid curves represent the best χ^2 fit obtained using the two resonance model described in the text. The integrated cross section (A_0) was simultaneously fitted. (Calarco *et al.*, 1977).

described above is valid, it provides a criterion for choosing the preferred solution. In this case the preferred solution is consistent with the results obtained from the DSD calculation previously presented, as well as with a microscopic calculation based on the doorway state model (Mavis, 1977).

The values of the best fit parameters are given in (Calarco *et al.*, 1977). It should be noted that the interaction strength parameter V was found to be in the range of 540–390 keV. Since the interaction strength due to isospin mixing is expected to be only ~ 150 keV (Mavis, 1977), the interpretation of this parameter is not clear. Further investigation of this point is clearly necessary.

This study emphasizes the utility of polarized proton capture measurements in unraveling the proton capture process and demonstrates the sensitivity of this reaction to the detailed intermediate structure of the GDR. Furthermore, the success of the above analysis supports the validity of the doorway state model, especially with regard to its use in interpreting the intermediate structure of ^{16}O in terms of n -particle n -hole configurations.

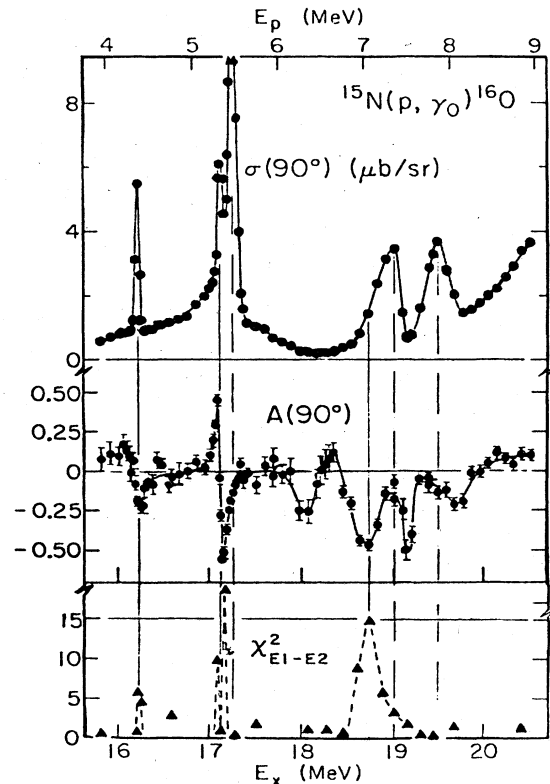


FIG. 7. The cross section σ and analyzing power A obtained at 90° and the reduced χ^2 for the angular distribution fits assuming only $E1$ and $E2$ radiation for the $^{15}\text{N}(p, \gamma)^{16}\text{O}$ reaction. The curves are to guide the eye. The vertical solid and dashed lines indicate $M1$ and $E1$ resonances, respectively (Snover *et al.*, 1979).

B. Polarized proton capture and $M1$ and $E2$ strength

In addition to the new information regarding $E1$ strength in radiative capture, polarized proton capture studies done in sufficient detail can be used to study $M1$ and/or $E2$ strength (Snover *et al.*, 1976, 1979; Weller *et al.*, 1974.) [In fact, some evidence indicating the presence of $E3$ radiation has been presented (Dietrich *et al.*, 1977).] For the case of $M1$ we shall discuss the recent study of magnetic dipole strength in ^{16}O (Snover *et al.*, 1979). In this work the $^{15}\text{N}(p, \gamma)^{16}\text{O}$ reaction was measured in the excitation energy region of 16 to 20 MeV. The results are shown in Fig. 7. The 90° analyzing power clearly deviates from zero, indicating the presence of radiations of opposite parity. When these data were analyzed assuming an $E1$ - $E2$ mixture, it was found that acceptable fits could not be obtained at certain energies. This is demonstrated in the χ^2 plot at the bottom of Fig. 7. However, when $M1$ radiation was included in the analysis, good fits were obtained. The results of this study are summarized in Table I. The 16.22-MeV resonance has been previously assigned 1^+ (Stroetzel and Goldman, 1970). The total $M1$ strength in ^{16}O ($\sim 0.24 \mu_N^2$) is a significant fraction of the known $M1$ strength in the neighboring $A = 4n$ nuclei (e.g., ^{12}C : $0.93 \mu_N^2$). Based on a comparison with the $2p$ - $2h$ states of ^{16}N (Ajzenberg-Selove, 1977), it ap-

TABLE I. 1^+ states in ^{16}O .

E_x (MeV)	Γ_{cm} (keV)	$\Gamma_p \Gamma_{\gamma_0} / \Gamma$ (eV)	Γ_p / Γ	Γ_{γ_0} (eV)	$B(M1) + (\mu_0^2)$
16.22 ^a	18 ± 3 ^a	2.65 ± 0.22	0.73 ^a	3.6 (5.1 ± 0.8) ^b	0.073 (0.103 ± 0.016) ^b
17.14 ^a	36 ± 5 ^a	3.75 ± 0.50	0.58 ^a	6.5	0.110
18.8	~250	>1.8 ± 0.3	≤0.5	≥3.6	≥0.047
Total					≥0.24 ^c

^a From Ajzenberg-Selove (1977).
^b From Stroetzel and Goldman (1970).
^c The two values for the 16.22-MeV state have been averaged.

pears that the $M1$ strength being observed in ^{16}O is built on the $2p$ - $2h$ ground-state correlations.

One of the first experiments which reported a possible $E2$ giant resonance in ^{16}O was due to Stewart *et al.* (1969) [see also Frederick *et al.* (1969)], who measured the angular distributions of the $^{16}\text{O}(\gamma, p_0)^{15}\text{N}$ reaction for photons of 21–32 MeV. These workers extracted the $E2$ cross section from these data by making some assumptions about the relative phases between the contributing T -matrix elements. Their results, shown in Fig. 8, indicate an $E2$ cross section which peaks near 26 MeV in ^{16}O and exhausts about 12.5% of the Gell-Mann-Telegdi isoscalar- $E2$ energy-weighted sum rule (IS- $E2$ -EWSR) [Gell-Mann and Telegdi (1953); see Appendix A].

Two recent experiments have been performed to investigate the $E2$ strength in ^{16}O utilizing polarized proton capture techniques. The advantage of these measurements over the previous work is, of course, the fact that the phases can now be determined from the data. The two experiments on the $^{15}\text{N}(p, \gamma)^{16}\text{O}$ reaction were performed at Stanford University (Hanna, 1979; LaCanna *et al.*, 1977) and at the University of Washington (Snover, 1979; Bussoletti, 1978). Both experiments consisted of obtaining cross section and analyzing power measurements of sufficient accuracy to enable the extraction of the coefficients A_0, a_1 through a_4 and b_1 through b_4 . Assuming that only $E1$ and $E2$ radiation contributes in the energy region of these experiments means that there are four T -matrix elements

to consider. Using the j - j coupling scheme and labeling these complex matrix elements by the orbital angular momentum brought in by the proton, we have

$$E1: se^{i\phi_s} \text{ and } de^{i\phi_d},$$

and

$$E2: pe^{i\phi_p} \text{ and } fe^{i\phi_f},$$

for the four matrix elements. Equations (17)–(19) of Sec. II can now be used to write the a_k and b_k coefficients in terms of these matrix elements:

$$1.0 = 0.75s^2 + 0.75d^2 + 1.25p^2 + 1.25f^2 \quad (\text{normalization})$$

$$a_1 = 2.372sp \cos(\phi_s - \phi_p) - 0.335dp \cos(\phi_d - \phi_p) + 2.465df \cos(\phi_d - \phi_f),$$

$$a_2 = 1.061sd \cos(\phi_s - \phi_d) - 0.375d^2 + 0.625p^2 - 0.437pf \cos(\phi_p - \phi_f) + 0.714f^2,$$

$$a_3 = 1.936sf \cos(\phi_s - \phi_f) + 2.012dp \cos(\phi_d - \phi_p) - 1.095df \cos(\phi_d - \phi_f),$$

$$a_4 = 3.499pf \cos(\phi_p - \phi_f) - 0.714f^2;$$

$$b_1 = 1.186sp \sin(\phi_s - \phi_p) - 0.671dp \sin(\phi_d - \phi_p) - 1.232df \sin(\phi_d - \phi_f),$$

$$b_2 = -0.530sd \sin(\phi_s - \phi_d) + 0.365pf \sin(\phi_p - \phi_f),$$

$$b_3 = -0.646sf \sin(\phi_s - \phi_f) + 0.671dp \sin(\phi_d - \phi_p) + 0.0913df \sin(\phi_d - \phi_f).$$

$$b_4 = -0.875pf \sin(\phi_p - \phi_f). \tag{34}$$

Efforts have been made to search for $M1$ effects in both of the previously mentioned data sets. For example, in the Stanford work (LaCanna *et al.*, 1977) the equations above were written so that a_1 and b_1 contained a term which represented $E1$ - $M1$ interference. This was justified, since, for $M1$ small compared to $E1$, $M1$ contributes only to a_1 and b_1 . The data were then fitted directly to the amplitudes and phases, bypassing the extraction of the a_k and b_k coefficients. Fits obtained with the term representing $E1$ - $M1$ interference set to zero and set free were compared, and it was concluded that there was no evidence for $M1$ radiation in the region of these measurements ($E_x = 19$ – 28 MeV). As mentioned above, however, $M1$ effects are observed just below this energy region. The resulting $E1$ and $E2$ T -matrix elements obtained by the Stanford group when possible $M1$ effects were excluded are shown in Fig. 9 (LaCanna *et al.*,

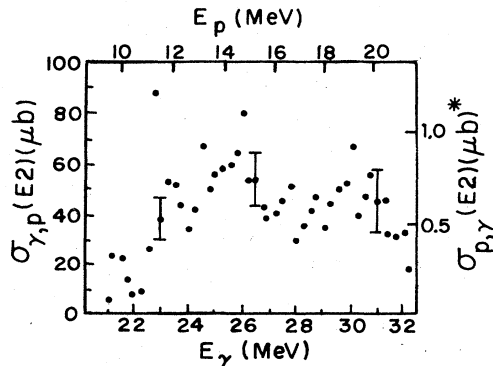


FIG. 8. The $E2$ cross section obtained for the $^{16}\text{O}(\gamma, p_0)^{15}\text{N}$ reaction. The (p, γ) cross section scale on the right was obtained using the detailed balance factor at $E_x = 27$ MeV (Stewart *et al.*, 1969; Frederick *et al.*, 1969).

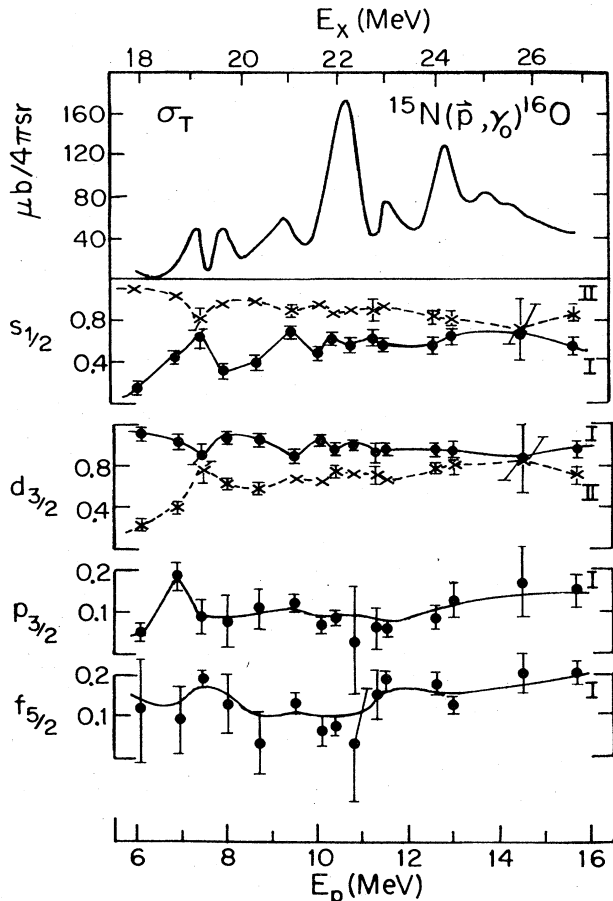


FIG. 9. The amplitudes of the $E1$ and $E2$ T -matrix elements extracted from the $^{15}\text{N}(p, \gamma_0)^{16}\text{O}$ data. Two solutions (labeled I and II) are found. Solution I is preferred (see text). The curves are to guide the eye. The error bars represent the statistical errors (La Canna, 1977).

1977). The result labeled Solution I corresponds to the case of primarily $d_{3/2}$ capture for the $E1$ strength which, as previously discussed, is the preferred solution.

The $E2$ cross section which follows from these results is shown in Fig. 10. These data suggest a possible $E2$ "resonance" at about 25 MeV ($E_p \sim 14$ MeV) which ex-

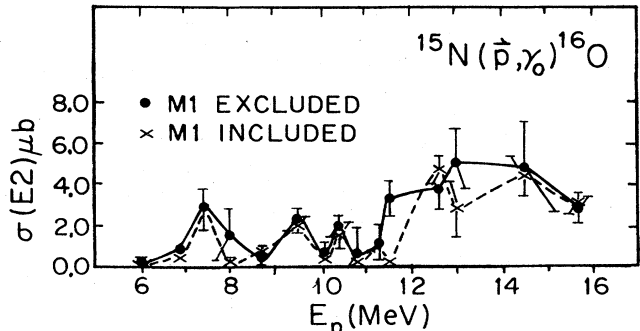


FIG. 10. The $E2$ cross section observed in the $^{15}\text{N}(p, \gamma_0)^{16}\text{O}$ reaction. The results corresponding to Fig. 9 are shown along with the results obtained when $M1$ radiation is included in the analysis (LaCanna, 1977).

hausts more than 20% of the IS-E2-EWSR (LaCanna *et al.*, 1977; Hanna, 1979). It can be seen from this figure that the results are essentially identical with and without the $M1$ radiation term in the a_1 and b_1 expressions. A comparison of these results with those of Frederick *et al.* (1969) (see Fig. 9) indicates that the new results show a substantially greater $E2$ cross section (E_p of 14 MeV corresponds to E_γ of ~ 25.25 MeV; $\sigma(p, \gamma)$ of $4.0 \mu\text{b}$ corresponds to $\sigma(\gamma, p)$ of $\sim 290 \mu\text{b}$). Both experiments suggest that the $E2$ cross section peaks in the vicinity of $E_x = 25$ MeV, significantly higher than both the predicted location of the isoscalar GQR in ^{16}O (Krewald *et al.*, 1974) and the isoscalar $E2$ strength observed in the (α, α') experiments (Knöpfle *et al.*, 1978). We will return to a discussion of these results after describing the second experimental study of this problem.

An independent study of this experiment has been performed at the University of Washington (Bussoletti, 1978; Snover, 1979). The technique of data taking and analysis were essentially identical to the Stanford procedure with one exception: the data were first fitted to obtain the a_k and b_k coefficients, which, in turn, were used to extract the T -matrix amplitudes and phases. The important point here is that the two techniques are identical if the errors are properly propagated. Snover (1979) and Bussoletti (1978) appear to have done so. The resulting $E2$ cross sections obtained in this

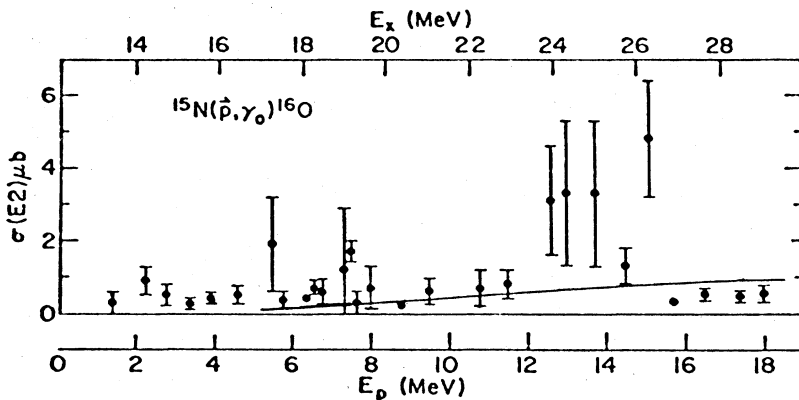


FIG. 11. The $E2$ cross section observed in the $^{15}\text{N}(p, \gamma)^{16}\text{O}$ reaction. All coefficients were included in obtaining these results. The solutions shown correspond to the $E1$ solution which is predominantly $d_{3/2}$ capture and should be regarded as the lower limit on the $E2$ strength in this channel. The solid curve is the result of a pure direct- $E2$ capture calculation (Snover, 1979; Bussoletti, 1978).

case are shown in Fig. 11. As in the previous case these results correspond to the dominant $d_{3/2}$ $E1$ solution. An analysis in which a_1 and b_1 were included and omitted in the data set indicated once again that $M1$ radiation is not necessary at these energies in ^{16}O . A detailed study of the solutions in χ^2 space revealed second solutions corresponding to somewhat larger $E2$ cross sections at many energies. Unfortunately, there seems to be no simple way to unambiguously choose one $E2$ solution over the other. The solutions shown in Fig. 11 correspond to the smallest $E2$ results found when a_1 and b_1 were included in the data set. They should be regarded as lower limits for the $E2$ cross sections.

The solid line on the $E2$ cross section parts of Fig. 11 is the result of a calculation which assumes that the $E2$ strength is entirely the result of direct capture (no collective state). This direct calculation describes the experiment fairly well with the exception of the possible bump near 25 MeV in ^{16}O . If the solutions are integrated over the energy range of the experiment (E_x of 13.4 to 29 MeV) it is found that they exhaust 20%–30% of the isoscalar $E2$ energy weighted sum rule. When these results are integrated over the energy range of the inelastic hadron experiment (E_x of 17.9–27.3 MeV) (Knöpfle *et al.*, 1978) it is found that they exhaust 12–22% of the IS–E2–EWSR. A summary of the $E2$ strength seen in this experiment is presented in Table II, where the results obtained from the direct $E2$ calculation are given along with the $E2$ strength obtained in the p_0 channel from the inelastic hadron experiment.

A detailed comparison of the two polarized proton capture experiments into ^{16}O indicates that, while there is qualitative agreement regarding the amount of $E2$ strength present in this channel, there are apparent discrepancies when the data are compared on a point for point basis. The quantity of data obtained by Bussoletti (1978) and Snover (1979) makes their conclusions appear to be more definitive than those of LaCanna (1977) and Hanna (1979). Therefore their conclusion that the (γ, p_0) cross section accounts for 12–22% of the IS–E2–EWSR in the region of 18 to 27, with some indication of a peak occurring near 25 MeV, should be accepted as the present result of these experiments.

Recent (α, α') experiments indicate that the isoscalar GQR is centered near 21 MeV in ^{16}O with a width of ~6 MeV and exhausts ~60% of the IS–E2–EWSR (Knöpfle *et al.*, 1975). Furthermore, coincidence studies (Knöpfle *et al.*, 1978) show that only ~9% of the IS–E2–EWSR is contained in the p_0 channel between 17.9 and 27.3 MeV, while 36% of the sum rule is in the α channel going to the first excited state of ^{12}C . Hence,

TABLE II. $E2$ strength in ^{16}O .

Energy interval in ^{16}O (MeV)	(p, γ_0) ^a	($\alpha, \alpha' p_0$)	Direct capture prediction
13.4–29	20–30	----	11
17.9–27.3	12–22	9	8

^a Assuming $\langle r^2 \rangle^{1/2} = 2.718$ fm (DeJager *et al.*, 1974).

the strength seen in the proton capture experiments appears to be in excess. It should be noted that Dehesa *et al.*, (1977) have suggested that the compact component of the isoscalar GQR in ^{16}O is primarily the $(p_{3/2}^- f_{7/2})$ configuration and offer this as a reason for not seeing this resonance in the $^{15}\text{N}(p, \gamma_0)^{16}\text{O}$ reaction, since the target is primarily $p_{1/2}^-$. Since isovector strength can be excited in the capture experiment, part of the strength seen could be of this nature. The isovector GQR is expected to lie at much higher energies, although it is possible that this strength is quite fragmented and makes a considerable contribution to the energy region being studied in the capture work (Paul, 1977). As previously mentioned, the direct $E2$ capture strength over the region of 17.9 to 27.3 MeV accounts for about 8% of the IS–E2–EWSR (Snover, 1979). Since the isoscalar and isovector effective charges are equal, these two components contribute equally to the capture strength. However, the factor which multiplies the cross section is proportional to the square of the total effective charge. Therefore, if a reaction selects *only* the isoscalar strength, it will contain only $\frac{1}{4}$ of the direct $E2$ strength (Snover, 1979). If we subtract this direct $E2$ strength from the $(\alpha, \alpha' p_0)$ strength, we obtain 7% of the IS–E2–EWSR, while if we subtract the full direct $E2$ strength from the capture experiment over the same energy region, we obtain 4%–14% of the sum rule. Therefore, we can conclude that, to within experimental uncertainties, the capture experiment, while “suggesting” an excess of strength over the $(\alpha, \alpha' p_0)$, does not disagree with the result of the $(\alpha, \alpha' p_0)$ experiment. However, there is some indication of an excess of $E2$ strength beyond that predicted for direct $E2$ capture in the region of 18–27 MeV. Of course, interference and mixing effects between the various $E2$ amplitudes must be considered in any quantitative analysis of these reactions.

Other studies of the region of the isoscalar $E2$ giant resonance using polarized proton capture have yielded results which are similar to those obtained in ^{16}O . The case of ^{15}N , studied via the $^{14}\text{C}(p, \gamma_0)^{15}\text{N}$ reaction (Snover *et al.*, 1976), was the first case in which it was pointed out that pure direct $E2$ capture gave a reasonably good description of the non- $E1$ effects in the data. DSD calculations which employed an $E1$ form factor proportional to the real-symmetry term in the optical-model potential and an $E2$ form factor proportional to the derivative of the central potential were performed for this case (Snover *et al.*, 1976). These calculations indicated that the effects of collective $E2$ strength were small and difficult to establish experimentally. Figure 12 shows the $E2$ cross section obtained in this work, along with the calculation for pure direct $E2$ capture. While the data from $E_x = 19.5$ to 27.0 MeV exhaust around 7% of the IS–E2–EWSR, the calculated direct capture cross section exhausts about 4% of this sum rule. The result of a DSD calculation which included the IS–GQR is also shown in Fig. 12. Clearly, the effects of the IS–GQR are predicted to be quite small in this channel. These $E2$ results are for the case of primarily $d_{3/2}$ $E1$ capture and were obtained with a_1 and b_1 included in the data set. Several energies showed second solutions with acceptable χ^2 cor-

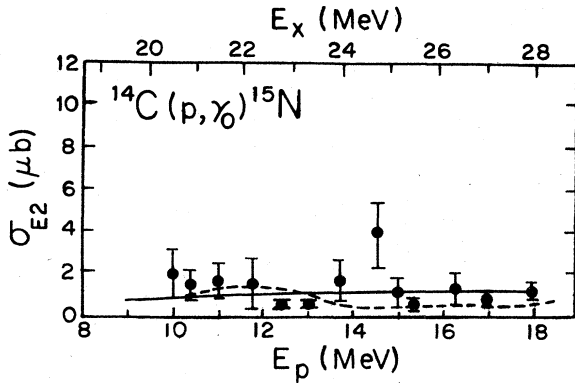


FIG. 12. The $E2$ cross section for the $^{14}\text{C}(p, \gamma_0)^{15}\text{N}$ reaction. These results correspond to the small $E2$ solution obtained using all measured coefficients. Several energies showed second solutions which corresponded to considerably larger $E2$ cross sections (4–10 μb). The error bars represent only the statistical errors. The solid curve is the result of a pure direct $E2$ capture calculation. The dashed curve includes an IS-E2-GQR in addition to the direct $E2$ component (Snover *et al.*, 1976).

responding to larger $E2$ cross sections, typically 4 to 10 μb . All of the solutions shown represent the small $E2$ solutions.

A recent study of the $^{13}\text{C}(p, \gamma_1)^{14}\text{N}(0^+, T=1)$ reaction also obtained similar results, as shown in Fig. 13 (Turner *et al.*, 1979). Here again there are two classes of solutions corresponding to primarily $d_{3/2}(E1)$ and primarily $s_{1/2}(E1)$ capture. The results shown are all for the primarily $d_{3/2}(E1)$ case, which is preferred on the basis of the DSD calculations. These $E1$ solutions are shown in Fig. 13 along with the results of a DSD calculation performed as described in Sec. IV.A. The dots and the x 's shown here correspond to two different acceptable minima in χ^2 . It can be seen that the $E1$ results (dots) corresponding to the smaller $E2$ solutions are in better agreement with the DSD calculation. Note that the larger $E2$ solutions (the x 's) do not exist at every energy. Furthermore, if the large $E2$ solution is integrated using the unique solution when appropriate, it is found to exhaust about 75% of the total (isoscalar plus isovector) $E2$ -EWSR in this one channel alone. Therefore, the small solution, which exhausts about 30% of the IS-E2-EWSR, is preferred. In this case we see that the direct $E2$ cross section, denoted by the solid curve in the top part of Fig. 13, can account for the observed $E2$ strength rather well without the addition of any other amplitudes, at least to within the accuracy of the experimental results and the certainty to which the direct $E2$ cross section can be calculated.

These results demonstrate how the polarized proton capture data allow us to extract useful physical information with a minimum of model dependent assertions. We have already seen that the $E1$ results for the relative amplitudes and phases could be accounted for with a simple DSD-E1 calculation. Now we have also demonstrated that being able to extract the $E2$ cross section from the experiment means that we can compare directly with the prediction of a pure direct $E2$ capture calculation. For this reason the reduction of the data to the T -matrix elements amplitudes and phases is clearly

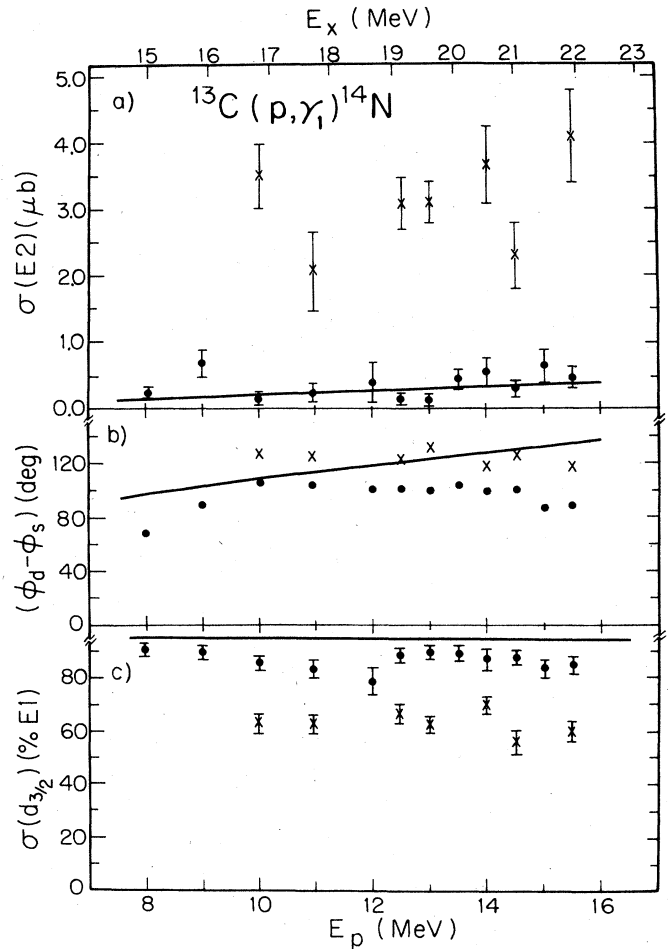


FIG. 13. (a) The $E2$ cross section observed in the $^{13}\text{C}(p, \gamma_1)^{14}\text{N}$ reaction. The x 's represent second solutions which were found at several energies. All solutions correspond to dominant $d_{3/2}(E1)$ results. The error bars are statistical errors. The solid curve is the result of a pure direct $E2$ calculation. (b) The relative phase between the two $E1$ amplitudes along with the result of the DSD calculation. The typical statistical error associated with these results is $\pm 4^\circ$. The x 's correspond to the large $E2$ solutions in (a). (c) The percentage of the $E1$ cross section due to $d_{3/2}(E1)$ capture along with the result of the DSD calculation. The x 's correspond to the large $E2$ solutions shown in (a). The error bars represent statistical errors only. The second solution (dominant s -wave capture) is not shown (Turner *et al.*, 1979).

more useful than simply reducing the data to a and b coefficients. Of course, a full description of the observations, especially the energy dependence of the $E1$ cross section, would require a more sophisticated calculation which could be compared to either amplitudes and phases or a and b coefficients.

In the three light nuclei which we have considered there is little convincing evidence for the presence of $E2$ strength which is clearly in excess of the amount predicted by a direct $E2$ calculation. The "peak" in the vicinity of 25 MeV in ^{16}O may be the exception. Calculations based on the DSD model indicate that the effect of the IS-GQR in the p_0 channel should be quite small—a result consistent with experimental findings. The con-

clusion we must draw from this is that polarized proton capture, at least in these nuclei, is not a particularly useful tool for studying the IS-GQR, at least not at the level of accuracy which has been achieved to date.

C. Polarized proton capture involving few nucleon systems

Polarized proton capture studies have also been applied to the three- and four-body problems through studies of the ${}^3\text{H}(p, \gamma){}^4\text{He}$ and the ${}^2\text{H}(p, \gamma){}^3\text{He}$ reactions (King, 1978; Skopik *et al.*, 1979). A discussion of the results of these experiments follows.

1. The ${}^3\text{H}(\vec{p}, \gamma){}^4\text{He}$ reaction

An investigation of the capture of polarized protons by tritium has been performed at Stanford University (Hanna, 1972; King, 1978). Angular distributions of cross section and analyzing power were measured at 7 or 8 angles in ~ 1.0 -MeV steps for proton energies ranging from 6 to 16 MeV. Using the LS coupling scheme, the T -matrix elements which contribute to this reaction in the cases of $E1$ and $E2$ radiation can be labeled by denoting the incoming partial waves (${}^{2S+1}L_J$) and the outgoing multipolarity. The four contributing complex T -matrix elements (T_{JS}) are expressed as

$$T_{10} = {}^1P_1 e^{i\phi_{1P}}(E1),$$

$$T_{11} = {}^3P_1 e^{i\phi_{3P}}(E1),$$

$$T_{20} = {}^1D_2 e^{i\phi_{1D}}(E2),$$

and

$$T_{21} = {}^3D_2 e^{i\phi_{3D}}(E2).$$

Note that the two $E1$ T -matrix elements correspond to the singlet ($S=0$) and the triplet ($S=1$) cases; the same is true for the two $E2$ matrix elements.

The coefficients of the expansion of $\sigma(\theta)/A_0$ (the a_k coefficients) and of the expansion of $A(\theta)\sigma(\theta)/A_0$ (the b_k coefficients) can be written in terms of the four T -matrix element amplitudes and the three relative phases using Eqs. (12) and (13) of Sec. II. The experiment provides nine measured coefficients: five a 's (including A_0 which will be normalized to 1.0) and four b 's, while there are seven unknowns. Since $M1$ radiation, if present, would be most important in the coefficients a_1 and b_1 , these can be left out in extracting the $E1$ and $E2$ amplitudes and phases, thereby reducing any possible error due to the neglect of $M1$ radiation. An analysis in which this was done yielded the relative amplitudes and phases shown in Fig. 14. The normalization was chosen so that:

$$0.75({}^1P_1^2 + {}^3P_1^2) + 1.25({}^1D_2^2 + {}^3D_2^2) = 1.0$$

at every energy.

The results shown in Fig. 14 indicate that the singlet P -wave amplitude remains almost constant over the entire energy range of the experiment, while the triplet P -wave amplitude appears to increase slightly with increasing energy. The D -wave amplitudes suggest a similar trend. The relative P -wave phase seems to be constant at about -50° , except at three energies which may be an experimental artifact. While the triplet $E1$

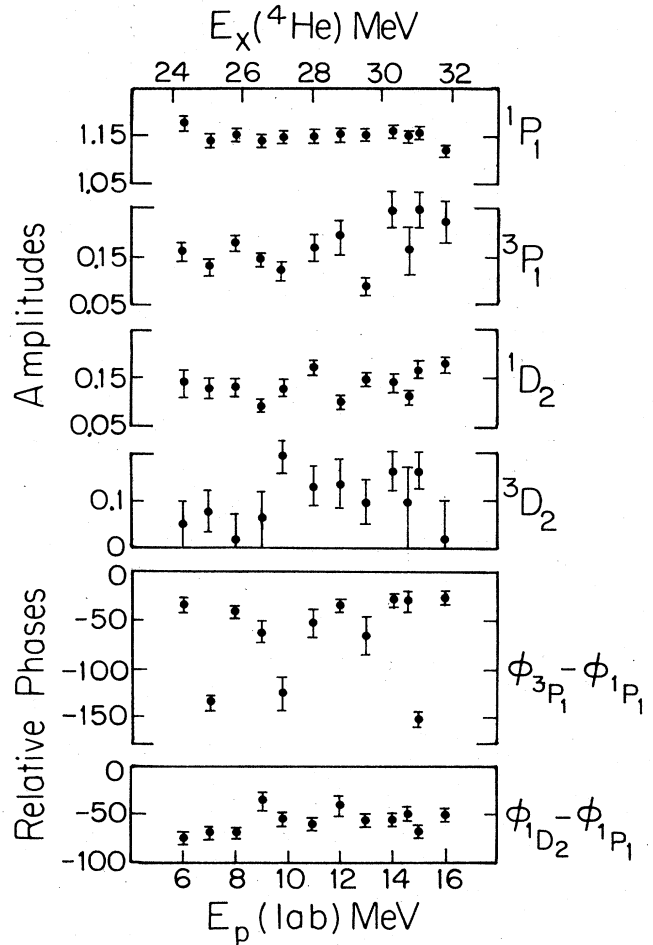


FIG. 14. The relative $E1$ and $E2$ amplitudes and the relative phases obtained for the ${}^3\text{H}(p, \gamma){}^4\text{He}$ reaction (King, 1978). The error bars represent the statistical errors associated with the data points.

amplitude accounts for about 1.5% of the total $E1$ cross section, the triplet $E2$ amplitude appears to be the same size as the singlet near $E_x = 28$ MeV. The large uncertainty in the triplet $E2$ amplitude indicates that further experimental confirmation of this surprising result is necessary.

Knowledge of the relative transition matrix elements can be combined with the experimentally determined absolute cross section to evaluate the $E1$ and $E2$ cross sections of the reaction. The results obtained in the present study are shown in Fig. 15, where the total (p, γ) cross section was obtained by normalization to the 90° results of Meyerhof *et al.* (1970) utilizing the expression $\sigma_T(p, \gamma) = \frac{1}{3}8\pi\sigma(90^\circ)$. These results are in reasonably good agreement with previous experimental measurements of the $E1$ and $E2$ cross sections for the ${}^3\text{H}(p, \gamma){}^4\text{He}$ reaction (Gemmell and Jones, 1962; Meyerhof *et al.*, 1970; Arkatov *et al.*, 1971).

A recent continuum shell model calculation (Halder-son and Philpott, 1979) has been published which appears to account for the analyzing power due to $E1$ radiation as observed in this experiment. This calculation demonstrates that the b_2 coefficient depends on the spin-orbit

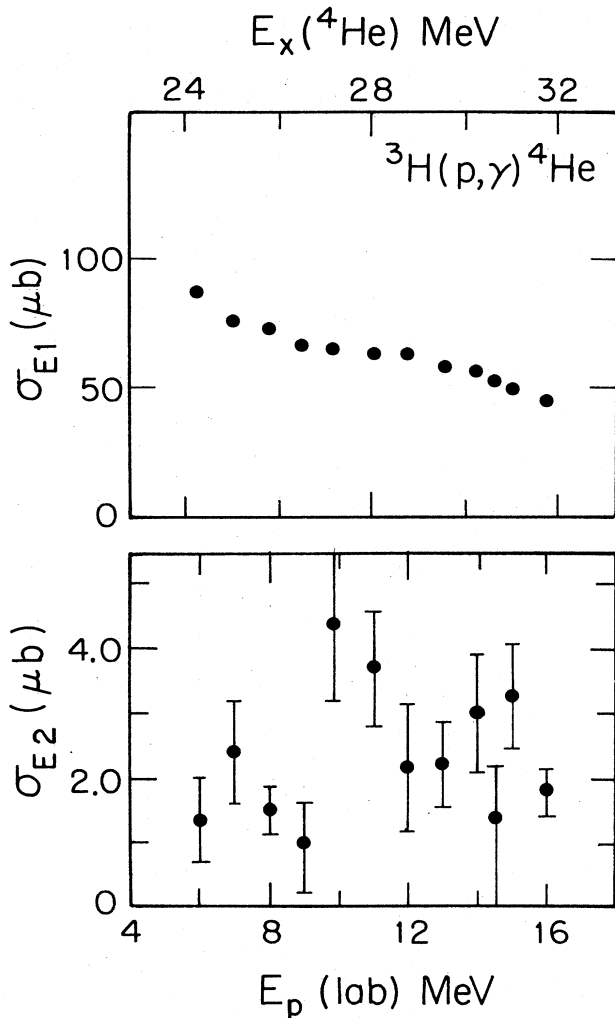


FIG. 15. The $E1$ and $E2$ cross sections obtained from the relative T -matrix elements of Fig. 14 but normalized to the 90° measurement of Meyerhof *et al.* (1970) (King, 1978).

odd component (LSO) of the effective nuclear force (Bertsch *et al.*, 1977). If one considers only the dominant $E1$ radiation, then b_2 can be written as:

$$b_2 = -0.707 {}^3P_1 {}^3P_1 \sin(\phi_{1P} - \phi_{3P}),$$

where

$$({}^3P_1)^2 + ({}^1P_1)^2 = 1.0.$$

These equations indicate that b_2 can arise from pure $E1$ radiation only if there is a finite contribution from the ${}^3P_1(E1)$ T -matrix element. The results of the calculation, which considered the ground state of ${}^4\text{He}$ to be an uncorrelated $S=0$ state, is shown in Fig. 16 for $E_p(\text{lab}) = 6.0$ MeV as a function of the (LSO) force strength. The value of 1.0 corresponds to the value of the LSO strength prescribed by Bertsch *et al.* (1977) and is seen to predict the observed b_2 value remarkably well. It should be noted that although the effects of $E2$ contributions to b_2 have not been considered in this calculation, these effects should be extremely small since they

would contribute to b_2 through a product of the $S=0$ and $S=1$ $E2$ T -matrix elements.

2. The ${}^2\text{H}(\bar{p}, \gamma){}^3\text{He}$ reaction

Polarized proton capture has also been investigated for the case of protons on deuterons (Skopik *et al.*, 1979). As in the ${}^3\text{H}(p, \gamma){}^4\text{He}$ case, the measured angular distributions of cross sections and analyzing powers were used to extract information on the amplitudes and phases of the contributing T -matrix elements. In this case there are two $E1$ and two $E2$ T -matrix elements for $S=1/2$. Denoting the incoming partial waves by ${}^{2S+1}L_J$, these are

$${}^2P_{1/2} e^{i\phi_{1/2}P}(E1),$$

$${}^2P_{3/2} e^{i\phi_{3/2}P}(E1),$$

$${}^2D_{3/2} e^{i\phi_{3/2}D}(E2),$$

and

$${}^2D_{5/2} e^{i\phi_{5/2}D}(E2).$$

It can be seen that in this case one has two $E1$ amplitudes without introducing the spin-flip amplitudes ($S=3/2$ terms). Hence the data were analyzed to determine the four amplitudes and the three relative phases of the $S=1/2$ T -matrix elements listed above. The results of the analysis of angular distribution data measured at $E_p = 5.0, 6.5,$ and 8.0 MeV are given in Table III. These results indicate that the two $E1$ matrix elements have amplitudes which are equal to within $\sim 5\%$, and that the two $E2$ matrix elements have amplitudes which are equal to within $\sim 10\%$, the differences being within the statistical uncertainties. Furthermore, while the relative phase between the two $E1$ or the two $E2$ matrix elements is only a few degrees with an error of comparable size, the $E1$ - $E2$ phase is about $\pm 80^\circ$, indicating that a plane wave approximation—which would predict 0° —is a poor one.

Under the assumptions of the analysis of Skopik *et al.* (1979), the results obtained here can, as in the ${}^3\text{H}(p, \gamma){}^4\text{He}$ case, be combined with the measured absolute cross section to obtain the $E1$ and the $E2$ cross sections. In this case an $E2$ cross section of $12 \pm 5\%$ of the $E1$ cross section was obtained. This corresponds to a total $E2$ cross section near 11 MeV in ${}^3\text{He}$ of $120 \pm 25 \mu\text{b}$, a value considerably larger than the published calculated value (Barbour and Hendry, 1972).

These polarized capture measurements have shown us that the capture of protons by deuterons proceeds as though there were one $E1$ amplitude and one $E2$ amplitude with a relative phase of about $\pm 80^\circ$. The ambiguity in the sign of the phase results from the fact that there are two solutions. The rather large $E2$ cross section which results when one assumes only non-spin-flip $E1$ and $E2$ amplitudes is in disagreement with the calculated values. Of course, the spin-flip terms as well as other multipoles could be important here. It also appears that the calculation may seriously underestimate the $E2$ cross section because the authors did not include the tensor force (Barbour and Hendry, 1972). This force is necessary in order for the $E2$ operator to connect the ${}^3\text{He}$ ground state with the large $l=0$ $p-d$ scattering states. Because of the strong

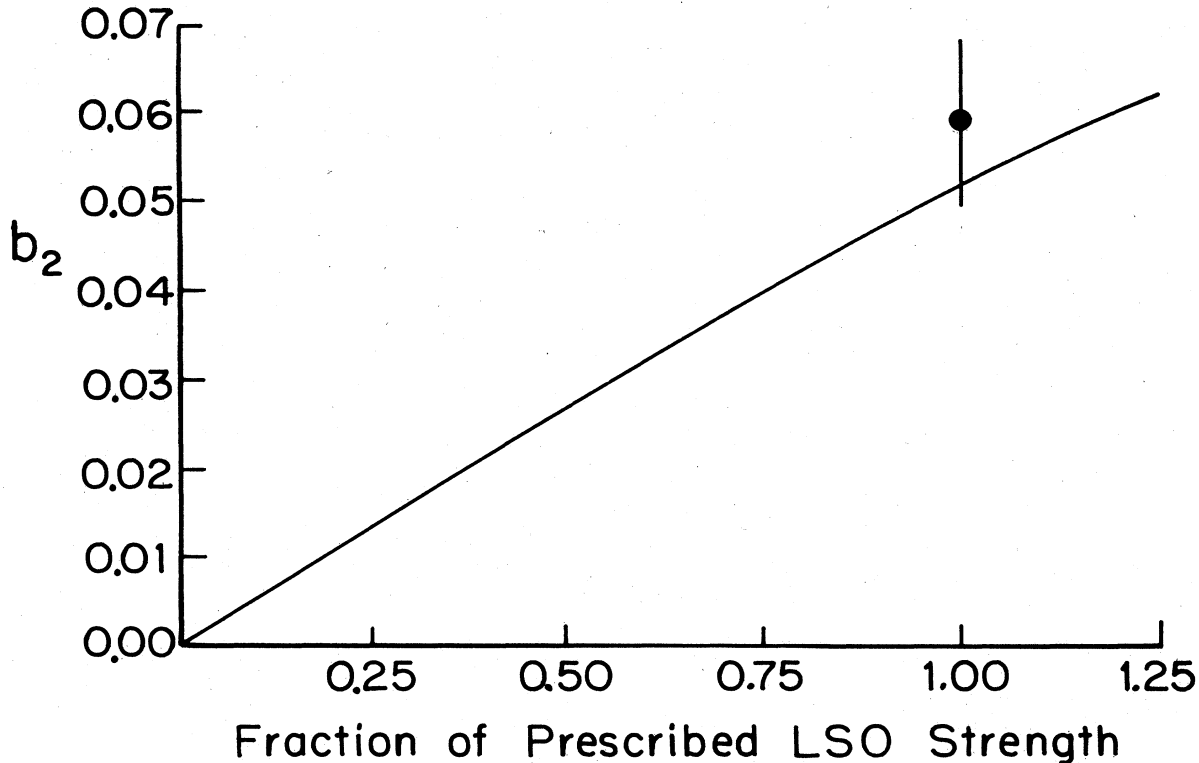


FIG. 16. The calculated value of the b_2 coefficient as a function of the fraction of the prescribed spin-orbit odd component of the effective nuclear force. The results shown are for $E_p(\text{lab}) = 6.0$ MeV; the data point is from King (1978) and has been plotted at the prescribed LSO strength (Halderson and Philpott, 1979).

interaction in the scattering states, this omitted transition may make a substantial contribution to the $E2$ cross section. An investigation of this point is presently underway (Gibson, 1979).

D. $E2$ strength and polarized neutron capture

As has been seen in previous examples, the presence of direct $E2$ strength presents a serious problem in the case of polarized proton capture studies since it can dominate the $E2$ reaction cross section and obscure any additional $E2$ strength which may be present. This problem, as has been discussed by several authors (Arthur *et al.*, 1975; Wender *et al.*, 1978), can be circumvented by studying neutron capture rather than proton capture. Since the direct capture amplitude is scaled by the recoil effective charge of the system, it is essentially eliminated in the case of neutron cap-

ture. For example, if one considers the case of protons on ^{14}N versus neutrons on ^{14}N the direct $E2$ amplitude will be down by a factor of about 30 for neutrons compared to protons.

Several experiments have been reported which show evidence for the presence of non- $E1$ radiation in fast neutron capture cross sections. The quantity usually reported is the fore-aft asymmetry:

$$a_s = \frac{Y(55^\circ) - Y(125^\circ)}{Y(55^\circ) + Y(125^\circ)} \cong 0.57a_1 - 0.38a_3,$$

where the last relationship, which relates the asymmetry to the coefficients of a Legendre polynomial expansion, requires the a_4 coefficient to be negligible.

One of the first published reports of a nonzero asymmetry was for the case of $^{88}\text{Sr}(n, \gamma)^{89}\text{Sr}^*$ (Likar *et al.*, 1978). In this work the γ rays leading to the final $3s_{1/2}$

TABLE III. Amplitudes and phases found for the $^2\text{H}(p, \gamma)^3\text{He}$ reaction. The fits were constrained such that $\sigma(0^\circ)$ and $\sigma(180^\circ)$ are zero with errors typical of those at other angles.

E_x (MeV)	$^2P_{1/2}$	$^2P_{3/2}$	$^2D_{3/2}$	$^2D_{5/2}$	$\phi_{3/2P} - \phi_{1/2P}$ (deg)	$\phi_{3/2D} - \phi_{1/2P}$ (deg)	$\phi_{5/2D} - \phi_{1/2P}$ (deg)
8.83	3.81 ± 0.13	3.97 ± 0.10	0.88 ± 0.14	0.94 ± 0.09	-2 ± 3	75 ± 5	82 ± 3
	3.87 ± 0.07	3.91 ± 0.06	1.01 ± 0.12	1.29 ± 0.07	-3 ± 1	-83 ± 3	-83 ± 3
9.83	3.74 ± 0.13	3.87 ± 0.10	1.04 ± 0.12	1.13 ± 0.76	-3 ± 2	81 ± 5	84 ± 3
	3.87 ± 0.07	3.81 ± 0.03	1.17 ± 0.11	1.07 ± 0.08	-3 ± 0.5	-87 ± 2	-86 ± 3
10.83	3.67 ± 0.14	3.91 ± 0.10	1.10 ± 0.23	1.09 ± 0.15	-1 ± 1	70 ± 10	77 ± 3
	3.94 ± 0.06	3.78 ± 0.07	1.14 ± 0.11	1.06 ± 0.08	-3 ± 1	-81 ± 2	-74 ± 1

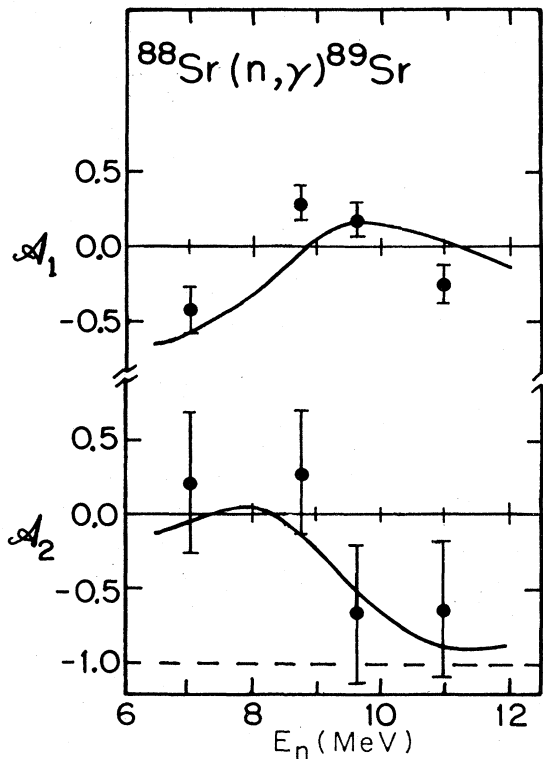


FIG. 17. Angular distribution coefficients α_1 and α_2 (see text) for γ rays leading to the $3s_{1/2}$ states for the reaction $^{88}\text{Sr}(n, \gamma)^{89}\text{Sr}$. The solid curves for α_2 is the result of a DSD calculation which includes the isoscalar GQR. The curve shown for α_1 represents a phenomenological fit which allows for the presence of a GQR (Likar *et al.*, 1978).

state in ^{89}Sr were not fully resolved, so that the experimental results remain to be confirmed. The results are shown in Fig. 17, where the coefficients

$$\alpha_1 = a_s \quad \text{and} \quad \alpha_2 = 2 - 4Y(90^\circ) / [Y(55^\circ) + Y(125^\circ)]$$

are plotted. These data show one point at $E_n = 7$ MeV which suggests a large effect. The solid curve for α_2 is the result of a DSD calculation which includes the isoscalar GQR. In the case of α_1 the solid curve is the result of a phenomenological fit which assumes the presence of a GQR (Likar *et al.*, 1978).

A more thorough experimental study has been performed for the case of $^{40}\text{Ca}(n, \gamma)^{41}\text{Ca}$ (Wender *et al.*, 1978). This study also consisted of measuring the fore-aft asymmetry as a function of neutron energy. The γ -ray spectrum obtained in this work was of sufficient quality to resolve the γ -ray leading to the ground state of ^{41}Ca . A typical spectrum was shown in Fig. 3 (Sec. III). The results of this study are shown in Fig. 18. The asymmetries are clearly not zero in the region of $E_n = 10$ MeV, the approximate energy ($E_x \sim 18$ MeV) at which the isoscalar $E2$ giant resonance is expected (Moss *et al.*, 1974; Youngblood *et al.*, 1976).

A DSD calculation using a complex form factor for $E1$ (Potokar, 1973) and a surface peaked form factor for $E2$ (Snover *et al.*, 1976) was performed for the $^{40}\text{Ca}(n, \gamma)^{41}\text{Ca}$ reaction. Compound nucleus contributions, expected to be small in this energy region, (Bergqvist and Potokar, 1979), have been ignored. The

results are shown in Fig. 18 (Wender *et al.*, 1978). Note that in this case the calculated asymmetry is zero if only direct $E2$ radiation is added to the dominant $E1$ strength. This is shown by the dashed line in the a_s part of Fig. 18. The other dashed lines in this figure are the results of a pure direct $E1$ calculation. The two solid curves labeled a and b in the 90° cross section plot are for two different parameter sets in the complex DSD coupling interaction [see Wender *et al.* (1978)]. The parameters used for the isoscalar GQR were $E_{\text{res}} = 18.0$ (18.2) MeV and $\Gamma = 4.0$ (2.2) MeV for curves 1 (and 2) of Fig. 18. (Youngblood *et al.*, 1977; T. Yamagata *et al.*, 1978.) The conclusion which can be drawn from these calculations is that when reasonable parameters are used, e.g., parameters which are consistent with other experimental results, and the isoscalar GQR is included, the calculated asymmetries are in reasonable agreement with the measured asymmetries. As has been previously argued, it is the virtual elimination of the direct $E2$ capture amplitude which increases the sensitivity of this experiment to non-direct (collective) $E2$ strength relative to proton capture studies of comparable precision.

One additional example which demonstrates the effect of direct $E2$ radiation rather dramatically is found in the case of $^{14}\text{N}(n, \gamma)^{15}\text{N}$ (Wender *et al.*, 1980). In this experiment measurements were made to determine the angular distribution expansion coefficients a_1 and a_2 in the region of the GDR. The results are shown in Fig. 19 along with the a_1 and a_2 coefficients obtained from the $^{14}\text{N}(p, \gamma)^{15}\text{O}$ reaction (Kuan *et al.*, 1970) and the $^{14}\text{C}(p, \gamma)^{15}\text{N}$ reaction (Bussoletti, 1978; Weller *et al.*, 1976; Harakeh *et al.*, 1975). Here we see that the rather large a_1 coefficient observed in both of the proton capture experiments has essentially vanished in the neutron capture reaction. This result is as expected if the a_1 coefficient in the proton capture cases arises primarily from interference of the DSD $E1$ radiation with direct $E2$ radiation. Note that the magnitude of the a_2 coefficient, which is determined primarily by the $E1$ strength, is not so different for the cases of neutron and proton capture.

Neutron capture studies have recently been greatly enriched by the production of rather high intensity beams of highly polarized neutrons (Jensen *et al.*, 1979). The polarized neutron beam was produced by using the $^2\text{H}(d, n)^3\text{He}$ reaction with a polarized deuteron beam of about 200 nA on target. The deuterium target consisted of a 3.0 cm long gas cell which was pressurized to about 3.0 atm. The neutron polarization was calculated from the measured incident deuteron beam polarization (p_3 and p_{33}) using the previously reported polarization transfer coefficients (K_y') and the tensor analyzing power (A_{zz}) of Lisowski *et al.*, (1975). The neutron polarization at zero degrees is given by

$$p_{y'}(0) = \frac{\frac{3}{2} p_3 K_y'(0)}{1 - \frac{1}{4} p_{33} A_{zz}(0)}$$

With values of $p_3 = p_{33} \sim 0.70$, $K_y'(0) \sim 0.64$, and $A_{zz}(0) \sim -0.46$ we obtain a value of 0.62 for the neutron polarization. A summary of the features which make this reaction particularly attractive is given below:

- (1) The $^2\text{H}(d, n)^3\text{He}$ reaction produces reasonably

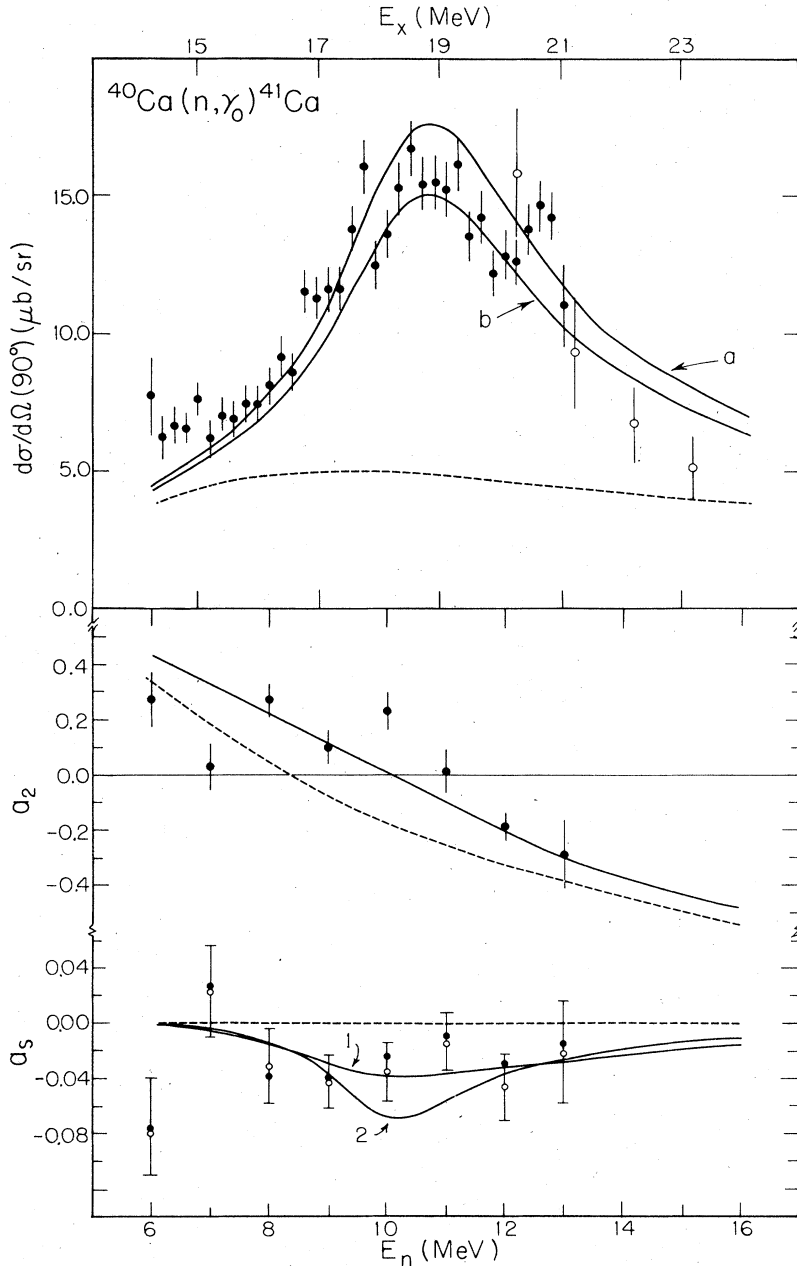


FIG. 18. The $^{40}\text{Ca}(n, \gamma)^{41}\text{Ca}$ reaction. The 90° yield curve data are shown along with the a_2 and a_3 coefficients (Wender *et al.*, 1978). The open circles in the a_3 data result from third-order fits while the solid circles are the result of second-order fits. The solid curves are the results of DSD calculations. The dashed curves for the yield curve data and the a_2 coefficients result from a calculation assuming pure-direct $E1$ capture. The dashed curve for a_3 assumes DSD dipole terms and direct $E2$ capture. Curves labeled 1 and 2 correspond to two different choices of the GQR parameters (see text).

intense monoenergetic neutron beams in the region of E_n of 5 to 18 MeV (Drosg and Drake, 1974). This energy range usually allows one to cover the GDR region.

(2) The neutron beam produced by this reaction is forward peaked (the yield typically falls to the $\sim 10\%$ level at an angle of 20° with respect to the beam) and reasonably intense (a flux of 10^8 neutrons/sr/sec is typical).

(3) The polarization transfer coefficient is large (about 90% of the incident beam polarization is transferred to the neutron) and almost constant over the energy range being discussed, varying from ~ 0.64 to ~ 0.62 for neutron energies of 6–14 MeV.

(4) The d beam producing this reaction can be pulsed so that a time-of-flight criterion can be used to eliminate many n induced events in the detector.

The reaction $^{40}\text{Ca}(n, \gamma)^{41}\text{Ca}$ has been studied at $E_n = 10$ MeV using a dc polarized neutron beam produced as just described, a 25.4×25.4 cm NaI spectrometer system, and a 3.8×3.8 cm right circular cylindrical sample of ^{40}Ca (Jensen *et al.*, 1979). The results are shown in Fig. 20. The expansion coefficients a_k and b_k are given in Table IV. These data clearly show non- $E1$ effects in both the cross section (backward peaking) and the analyzing power [$A(90^\circ + \theta) \neq -A(90^\circ - \theta)$] measure-

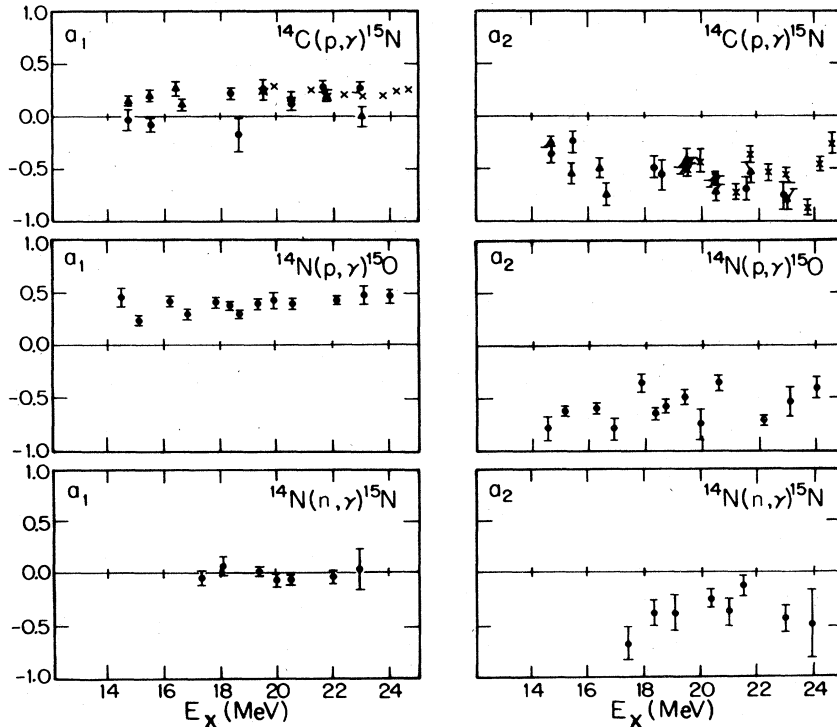


FIG. 19. The a_1 and a_2 coefficients for the $^{14}\text{C}(p, \gamma)^{15}\text{N}$, [(●) Weller *et al.*, 1976; (x) Bussoletti, 1978; (▲) Harakeh *et al.*, 1975], $^{14}\text{N}(p, \gamma)^{15}\text{O}$ (Kuan *et al.*, 1970) and $^{14}\text{N}(n, \gamma)^{15}\text{N}$ (Wender *et al.*, 1979) reactions.

ments. Although these data have not been corrected for multiple scattering and finite geometry effects, it has been determined that these effects are relatively small. This was done by use of a Monte-Carlo computation for the case of the cross section data. In the case of the analyzing powers, measurements using smaller targets

and the $^{12}\text{C}(n, n'\gamma)$ reaction indicate that the corrections will be less than the statistical errors associated with the data points, although a detailed evaluation of these effects remains to be performed.

Unfortunately, the final-state spin of ^{41}Ca makes a model-independent analysis in terms of $E1$ and $E2$ T -matrix elements impossible in this case. However, by using the DSD model it is possible to choose two $E1$ terms and two $E2$ terms which should account for all but a few percent of the strength in each multipole. In the j - j scheme the important $E1$ terms correspond to $g_{9/2}$ or $d_{5/2}$ neutron capture, while the relevant $E2$ terms correspond to $f_{7/2}$ or $h_{11/2}$ capture if the form factor is taken to be proportional to r^2 . Following the procedures used in polarized proton capture, the data were fitted to the four amplitudes and the three relative phases of these four T -matrix elements. The resulting fits to the cross section and analyzing power data are shown as the solid curves in Fig. 20.

The results of this $E1$ - $E2$ analysis for the $E1$ terms are shown in Fig. 21, where the results of analyzing less extensive measurements at three other neutron energies are also included. Note that, as in p capture, there are two solutions: one corresponding to pri-

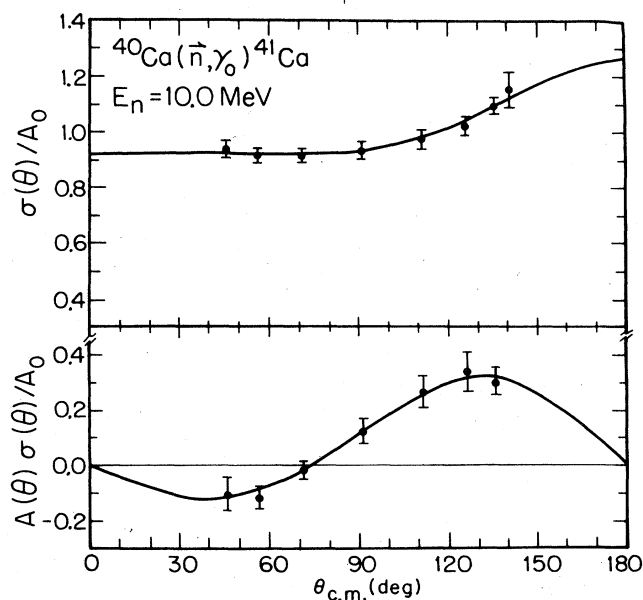


FIG. 20. The cross section and analyzing power as a function of angle for the $^{40}\text{Ca}(n, \gamma)^{41}\text{Ca}$ reaction at $E_n = 10.0$ MeV. The error bars represent statistical errors. The smooth curves were generated by fitting the data to the T -matrix amplitudes and phases described in the text (Jensen *et al.*, 1979).

TABLE IV. Expansion coefficients obtained for the 10 MeV $^{40}\text{Ca}(n, \gamma)^{41}\text{Ca}$ data of Fig. 21.

a_1	-0.13 ± 0.03
a_2	0.11 ± 0.03
a_3	-0.05 ± 0.05
b_1	0.13 ± 0.02
b_2	-0.15 ± 0.02
b_3	0.00 ± 0.02

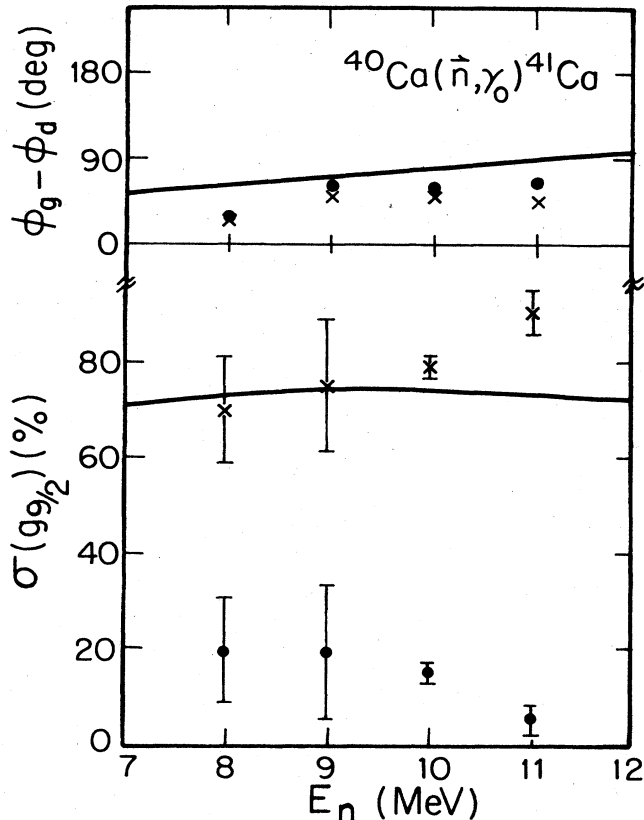


FIG. 21. The results of the T -matrix element analysis of the $^{40}\text{Ca}(n, \gamma)^{41}\text{Ca}$ data for the $E1$ terms. The two solutions are shown as the o 's and x 's. The amplitude results are plotted as the percent of the cross section which is due to the $g_{9/2}$ neutron capture amplitude. The remaining $E1$ strength corresponds to $d_{5/2}$ neutron capture. Statistical errors are indicated; the errors associated with the phase differences are typically $\pm 10^\circ$. The solid lines are the result of the DSD calculation described in the text.

marily $g_{9/2}$ capture, the other to primarily $d_{5/2}$ capture. The solid curves are the result of a direct capture calculation (or DSD with a form factor αr). Clearly, this calculation picks the solution which corresponds to primarily $g_{9/2}$ capture.

The $E2$ T -matrix elements for the $E_n = 10$ MeV results are, in terms of percentage contributions to the total cross section, $f_{7/2}$: $2.1 \pm 2.7\%$ and $h_{11/2}$: $1.2 \pm 0.4\%$. The $E2$ cross section at $E_n = 10$ MeV turns out to be $3.3 \pm 2.7\%$ of the total cross section. If we use the position and width of the isoscalar $E2$ resonance in ^{40}Ca as determined by the (α, α') measurements (Youngblood *et al.*, 1977), and assume that the $E2$ strength obtained in the present experiment is isoscalar, then this result implies that $\sim 3\%$ of the $E2$ -IS-EWSR would be present in the ground-state neutron channel of ^{41}Ca .

The value of these polarized neutron capture measurements seems evident. The sensitivity of the analyzing power to the presence of (nondirect) $E2$ radiation appears to be much greater than the fore-aft asymmetry, besides being experimentally more dependable [measuring 5% asymmetries in $\sigma(\theta)$ requires extremely

good knowledge of the background which, in general, will vary with the detector angle]. It is significant that coherent $E2$ radiation is observed here. That is, the $E2$ T -matrix element clearly has a definite phase relation with respect to the $E1$ terms, as evidenced by the finite a_1 and b_1 coefficients. Since this $E2$ strength is not direct, this result implies that the GQR is decaying in a nonstatistical manner into the ground state neutron channel. So we can conclude that statistical compound nucleus contributions are relatively unimportant here. Unfortunately, a positive identification of this $E2$ strength with the isoscalar GQR is still lacking.

The $E2$ solutions obtained above indicate a large uncertainty in the $f_{7/2}$ strength, almost overlapping zero. This is apparently a result of the nonlinear nature of the relevant equations more than the statistical errors in the data. The DSD calculation performed here indicates that the $h_{11/2}$ $E2$ term will account for $\sim 85\%$ of the $E2$ cross section. If the $E_n = 10$ MeV data are fitted with only the $h_{11/2}$ $E2$ T -matrix element and the two $E1$ terms previously discussed, an acceptable fit (χ^2) is obtained. This result indicates that the $h_{11/2}$ $E2$ term accounts for $1.3 \pm 0.4\%$ of the total cross section. What is interesting here is that under this situation the b_1 expression contains only one term:

$$b_1 = -6.65 g_{9/2} h_{11/2} \sin(\phi_h - \phi_g).$$

Furthermore, the solution indicates that $\sin(\phi_h - \phi_g) = 0.96$. Since the phase factor is ~ 1.0 , we cannot obtain the experimental value of b_1 by having a smaller $E2$ strength (supposing part of it were incoherent and therefore not contributing to b_1) and a compensating variation in the phase difference. So we see that almost all of the $h_{11/2}$ strength must be coherent. Of course, it is important to remember that although the DSD calculation supports the interpretation of the non- $E1$ strength as $E2$ -strength, the observations alone (finite a_1 and b_1) do not rule out the possibility of $M1$ strength, which has been ignored here.

Some of the conclusions which can be drawn from this polarized neutron capture experiment are listed below:

- (1) The $E1$ cross section for the $^{40}\text{Ca}(n, \gamma)^{41}\text{Ca}$ reaction is dominated (70–85%) by $g_{9/2}$ neutron capture in the region of the GDR.
- (2) There is non- $E1$ radiation present in the fast neutron capture reaction on ^{40}Ca .
- (3) If this radiation is assumed to be $E2$, the data can be fitted if the $E2$ strength is 1–3% of the total.
- (4) If we apply the isoscalar GQR parameters for ^{40}Ca from the (α, α') experiments to the present case, the $E2$ strength seen here would correspond to about 1–3% of IS- $E2$ -EWSR in the n_0 channel for ^{41}Ca .
- (5) The $E2$ strength appears to be almost entirely coherent with respect to the $E1$ strength and therefore "semidirect."

The study of polarized neutron capture has just begun. Clearly, many important questions can be addressed with this technique. Future experiments where the spin situation is more favorable (e.g., a spin-zero final state) should provide more model independent results and allow for a more thorough examination of the role of $M1$ radiation in these reactions.

E. Alpha capture and E2 strength

Perhaps the most convincing observation of the GQR in an alpha capture experiment is the case of $^{12}\text{C}(\alpha, \gamma_0)^{16}\text{O}$ (Snover *et al.*, 1974), where 17% of the IS-E2-EWSR was observed between E_x of 12 to 28 MeV. In this case qualitative agreement was obtained between the shape of the E2 strength seen in this reaction and the results of the coincidence decay study of the isoscalar GQR via the $^{16}\text{O}(\alpha, \alpha'\alpha_0)$ reaction (Knöpfle *et al.*, 1978), as illustrated in Fig. 22. However, detailed comparisons of the absolute strengths seen in these two experiments [(α, γ) and $(\alpha, \alpha'\alpha_0)$] have indicated that the E2 strength seen in the capture experiment is about a factor of 2 to 4 smaller than that seen in the $(\alpha, \alpha'\alpha_0)$ experiment (Snover, 1979). It has been suggested that isospin impurities in the GQR and subsequent destructive interference between the IS and IV electromagnetic transition amplitudes in the (α, γ) reaction may be responsible for this result (Knöpfle, 1979).

A number of (α, γ) experiments have been performed on heavier target nuclei. These include $^{24,26}\text{Mg}$ (Meyer-Schützmeister *et al.*, 1968), $^{20,22}\text{Ne}$ (Kulmann *et al.*, 1975), $^{28,30}\text{Si}$ (Meyer-Schützmeister *et al.*, 1968; Kulmann *et al.*, 1979), $^{40,48}\text{Ca}$ (Peschel *et al.*, 1974), $^{38,40}\text{Ar}$ (Foote *et al.*, 1976), ^{48}Ti (Foote *et al.*, 1976), ^{36}Ar (Watson *et al.*, 1973), and ^{54}Fe (Meyer-Schützmeister *et al.*, 1978). In this paper we shall concentrate on two recent papers which directly address the

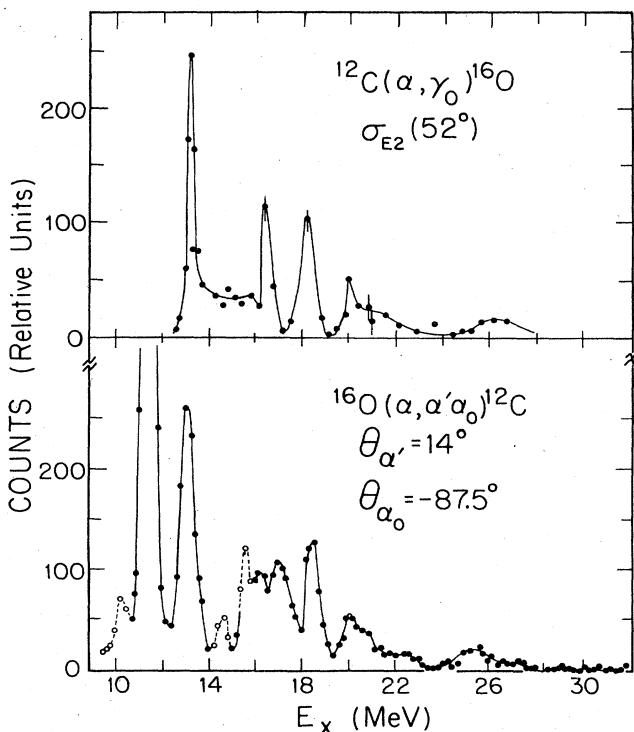


FIG. 22. The E2 cross section obtained from the $^{12}\text{C}(\alpha, \gamma_0)$ experiment is shown at the top (Snover *et al.*, 1974). The bottom shows the $^{16}\text{O}(\alpha, \alpha'\alpha_0)$ spectrum transformed to the $(\alpha + ^{12}\text{C})$ -cm system (Knöpfle *et al.*, 1978). The dashed parts denote non $L = 2$ strength as determined by the analysis of Knöpfle *et al.* (1978).

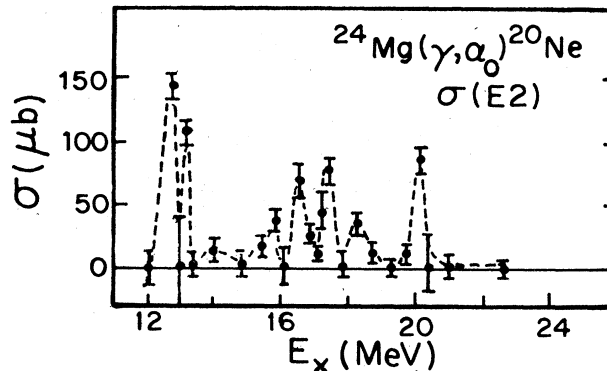


FIG. 23. The total E2 cross section extracted from the $^{20}\text{Ne}(\alpha, \gamma)^{24}\text{Mg}$ reaction and converted by detailed balance to that for the $^{24}\text{Mg}(\gamma, \alpha_0)^{20}\text{Ne}$ reaction. (Kulmann *et al.*, 1975.)

question of the E2 strength seen in this reaction.

The giant resonance regions of ^{24}Mg and ^{26}Mg were studied by measuring the (α, γ) reaction on targets of ^{20}Ne and ^{22}Ne as a function of energy and angle (Kulmann *et al.*, 1975). The E2 cross section was extracted from the angular distributions with the assumption that only E1 and E2 radiation are present. The result for ^{24}Mg is shown in Fig. 23. About 12% of the IS-E2-EWSR is contained in these data. Figure 24 displays the E2 strength given as the percentage of the IS-E2-EWSR integrated over 2-MeV intervals for both ^{24}Mg and ^{26}Mg . Bound states and low-lying resonances are included along with the strength observed in the α_0 decay channel. (Endt and Van der Leun, 1973; Lees *et al.*, 1974.) The arrows indicate the position of $63 A^{-1/3}$ MeV, i.e., the expected position of the isoscalar GQR (Bertrand 1976). It can be seen that almost 50% of the IS-E2-

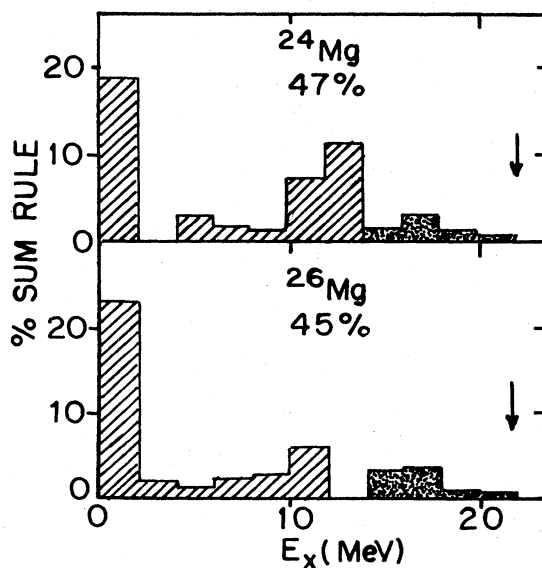


FIG. 24. Top: The E2 strength integrated over 2-MeV intervals (in percentage of the energy-weighted sum rule) in the bound states and low lying resonances and in the α_0 decay channel (stippled region) for ^{24}Mg . Bottom: Same for ^{26}Mg . The arrows indicate the expected position of the IS-GQR (Kulmann *et al.*, 1975).

EWSR strength is accounted for below $63 A^{-1/3}$ MeV.

Although no evidence for a narrow GQR was found in these experiments, a significant conclusion concerning the (α, γ_0) reaction mechanism was deduced. If it is assumed that the α capture reaction excites quadrupole strength only through a compound nucleus mechanism and that this strength subsequently decays in a purely statistical manner, then it is possible to derive the total absorption cross section for isoscalar $E2$ radiation $\sigma_{\text{TOT}}^{\text{CN}}(E2)$ from the measured $\sigma(\gamma, \alpha_0)$ cross section (Hauser and Feshbach, 1952; Foote *et al.*, 1974):

$$\sigma_{\text{TOT}}^{\text{CN}}(E2) = \left(\frac{T_{\alpha_0}}{\sum_i T_i} \right)^{-1} \sigma(\gamma, \alpha_0)_{E2},$$

where T_i denotes the transmission coefficient for decay into channel i . If this is done for the case of ^{26}Mg , it is found that the assumption of a purely compound process leads to $\sim 300\%$ of the sum rule strength. Hence it was concluded that there is a significant noncompound component in the (γ, α_0) $E2$ cross section for the case of ^{26}Mg . A similar analysis for the case of ^{24}Mg gave an integrated strength which was only slightly in excess of the sum rule. Therefore in this case it was concluded there was no convincing positive evidence for a noncompound component in $\sigma(\alpha, \gamma_0)_{E2}$ (Kuhlmann *et al.*, 1975).

The question can now be raised as to whether the angular distribution information is consistent with this conclusion. In both of these cases, it is observed that the relative $E1$ - $E2$ phase remains close to 90° . Indeed, as we go to heavier nuclei where the fluctuations in the cross section disappear (e.g., ^{58}Ni , see below), this phase factor gets even closer to being equal to 90° . It has been pointed out (Watson *et al.*, 1973) that if at least one of the multipoles excited in the capture reaction consists of a great number of overlapping resonances, then a phase averaging will occur, so that the interference term will vanish. Since statistical analyses have indicated that α capture into the isovector GDR proceeds predominantly through a statistical compound process (Meyer-Schützmeister *et al.*, 1968; Kuhlmann *et al.*, 1975), the above results are consistent with the 90° phase (i.e., $\cos 90^\circ = 0$ and so the interference term is zero). Namely, the $E2$ radiation which results from α capture could be nonstatistical, and one would not observe coherence with respect to the $E1$ radiation if the $E1$ strength is itself statistical in nature.

The final α capture measurement which we shall discuss is probably, with the exception of $^{12}\text{C}(\alpha, \gamma_0)^{16}\text{O}$, the most positive result to date. In the case of $^{54}\text{Fe}(\alpha, \gamma_0)^{58}\text{Ni}$ the angular distributions were used to extract the $E2$ strength under the assumption that only $E1$ and $E2$ radiation are present (Meyer-Schützmeister *et al.*, 1978). The resulting $E2$ cross section is shown as a function of excitation energy in Fig. 25. The $E2$ cross section appears to display a resonancelike behavior with a peak position near $63 A^{-1/3}$ MeV. It should be noted, however, that this behavior is influenced by the accidental proximity of the GQR to the α nucleus Coulomb barrier in this case. The GQR of ^{58}Ni has been previously observed in an (α, α') reaction

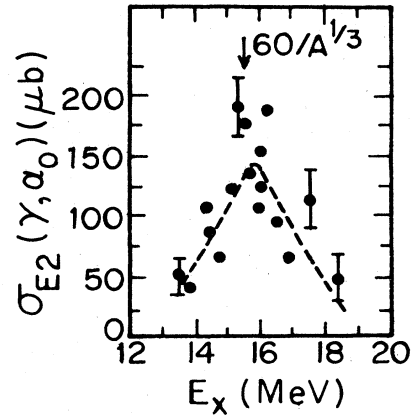


FIG. 25. The angle integrated $E2$ cross section deduced from the $^{54}\text{Fe}(\alpha, \gamma)^{58}\text{Ni}$ reaction is shown as a function of excitation energy in ^{58}Ni . It is plotted as $^{58}\text{Ni}(\gamma, \alpha_0)^{54}\text{Fe}$ cross section by the method of detailed balancing (Meyer-Schützmeister *et al.*, 1978).

study and found to exhaust $\sim 55\%$ of the $E2$ -IS-EWSR (Youngblood *et al.*, 1976). The measured $E2$ strength shown here corresponds to about 4% of the $E2$ -IS-EWSR. In this case, as previously mentioned, the phase difference between the $E1$ and $E2$ amplitude is close to being 90° over the entire range of the experiment.

For this case, as in the case of Mg , it is possible to calculate the total $E2$ absorption cross section from $\sigma(\gamma, \alpha_0)_{E2}$ and the transmission coefficients. The result of this calculation implies that 150% of the $E2$ -IS-EWSR would be exhausted in the measured energy region of ^{58}Ni (Meyer-Schützmeister *et al.*, 1978). Hence it is concluded that significant direct or semidirect components contribute to the α capture process into the GQR. Due to the rather large uncertainty in the capture experiment, this result remains somewhat uncertain. It should be noted that the results of a recent (α, α') coincidence experiment (Collins *et al.*, 1979) indicate a somewhat smaller α_0 decay strength ($< 3\%$ of the $E2$ -IS-EWSR). However, together with the results obtained from the $^{22}\text{Ne}(\alpha, \gamma)^{26}\text{Mg}$ reaction, as well as similar results obtained in ^{32}S and ^{34}S (Kuhlmann *et al.*, 1979), these capture experiments provide strong evidence for the fact that the $E2$ strength in the region of the IS-GQR does not decay into the α_0 channel in a purely statistical manner.

V. CONCLUSIONS

This review of some recent proton, neutron, and alpha capture measurements has attempted to show how these studies have revealed new insight into the nature of capture reactions, particularly on the basis of the angular distribution measurements. The polarized proton and neutron capture studies have shown us that the principle factor responsible for the energy dependence of the angular distributions (i.e., of the a_2 coefficient) is the relative phase between the two $E1$ transition matrix elements. The relative $E1$ amplitudes appear to be remarkably constant as we cross the GDR region. In the case of spin-zero targets, where the GDR has more than one possible J^π value, these results suggest

that there is no gross J splitting of the GDR. We have also seen that at least for light nuclei much of the observed behavior of the amplitudes and phases for both protons and neutrons can be predicted by a direct-semidirect calculation using a form factor proportional to r . This calculation appears to provide a dependable means for choosing between the two solutions which result from the analysis of the data.

Although the gross features which result from measuring the capture reactions with polarized beams do not appear to be sensitive to the structure of the GDR, we have seen that detailed measurements (e.g., the case of $^{15}\text{N} + \text{p}$) are sensitive to this structure and can be used to test our models. In the case of $^3\text{H}(\text{p}, \gamma)^4\text{He}$ we have seen that the b_2 coefficient appears to be quite sensitive to the spin-orbit odd component of the effective nuclear force. This is a case in which the virtues of *polarized* capture measurements are especially evident. The study of $\text{p} + d$ has shown us that the approximation that this reaction proceeds as though there is a single $E1$ and a single $E2$ amplitude is a good one. However, the neglect of $S = 3/2$ $E1$ and $E2$ amplitudes, as well as the neglect of higher multipoles, remains to be justified.

The comparison of proton and neutron capture studies seems to confirm the idea that the direct $E2$ amplitude is playing a significant role in the proton capture reaction. While the $E2$ strength observed in ^{16}O via proton capture appears to be somewhat in excess of that which is calculated assuming the presence of only direct $E2$ capture, other studies of nuclei near ^{16}O (e.g., ^{14}N and ^{15}N) do not necessarily require additional amplitudes in order to account for the observed $E2$ strength. Higher precision measurements at more energies could change this conclusion. While these studies have shown no evidence which indicates the presence of $M1$ radiation in the energy region of the GQR, polarized proton capture studies at somewhat lower energies have been able to identify $M1$ strength in the case of ^{16}O . Further investigations along these lines should be quite interesting.

The neutron capture study of ^{41}Ca seems to establish the presence of $E2$ strength which is not direct. The DSD model appears able to account for the observed total cross section and the angular distributions. These calculations used a complex form factor for the $E1$ strength

and a surface peaked form factor for the $E2$ strength. The success of these calculations supports the assumption of little or no $M1$ radiation made in the analysis of the data. Since the $E2$ strength observed here is being seen by virtue of its interference with the dominant $E1$ amplitudes, this observation verifies the presence of nonstatistical processes in the $E2$ transition strength other than direct capture. The experiment does not, however, distinguish between isoscalar and isovector $E2$ strength.

The α capture experiments also reveal $E2$ strength. However, in experiments performed to date the α_0 channel appears to be an important decay channel for the IS-GQR only in the case of ^{16}O . In cases where isolated resonance structure is not observed, the $E1$ and $E2$ amplitudes appear to be incoherent as evidenced by the fact that the angular distributions do not display a finite interference term. Since the IV-GDR is expected to be populated via statistical processes in the α capture reactions, this result does not tell us anything about the nature of the $E2$ component. However, in several cases it is found that Hauser-Feshbach calculations indicate that the amount of $E2$ strength observed in the experiments is too large to be accounted for by a purely statistical compound process.

It is hoped that further studies of α capture and especially polarized neutron capture will substantiate these initial results. It should be important to determine more quantitatively the fraction of the reaction which proceeds via nonstatistical processes. Clearly the study of intermediate structure, the study of giant resonances built on excited states, and a thorough investigation in the region of the isovector GQR are areas which should receive increased attention in the near future.

Note added in proof: The direct $E2$ calculation shown in Fig. 13 assumed a value of $C^2S = 1.7$ (not $S = 0.85$ as reported in Turner *et al.*, 1980). If a value of $C^2S = 0.85$ is used, the possibility of excess $E2$ strength near 20–22 MeV becomes somewhat more likely.

ACKNOWLEDGMENTS

The authors are indebted to all of their TUNL colleagues who contributed to many of the experiments described in this paper. In particular, they wish to thank

TABLE A1. $E2$ energy-weighted sum rules.^a

$\int \frac{\sigma(E2)dE\gamma}{E_\gamma^2}$	Comments and references
$= \frac{\pi^2}{137} \frac{A}{12} \frac{\langle r_p^2 \rangle}{938} \text{ fm}^2/\text{MeV}$	GMT (Gell-Mann and Telegdi, 1953) Pure isoscalar for self conjugate nuclei
$= \text{GMT} \times \frac{4Z^2}{A^2} \text{ fm}^2/\text{MeV}$	$\Delta T = 0$ (Nathan and Nilsson, 1965) (equals GMT above for $N = Z$)
$= \text{GMT} \times \frac{4NZ}{A^2} \text{ fm}^2/\text{MeV}$	$\Delta T = 1$ (Nathan and Nilsson, 1965)

^a $\langle r_p^2 \rangle$ represents the mean-squared moment of the charge radius. For a uniformly charged sphere of radius $R = 1.2A^{1/3}$ one has $\langle r_p^2 \rangle = \frac{3}{5} (1.2A^{1/3})^2$. The value of $\langle r_p^2 \rangle$ may also be taken from electron scattering data, if available.

Drs. Blue, Clegg, Cotanch, Rickel, Seyler, Tilley, and Wender for their essential contributions to the TUNL capture program.

APPENDIX A: E_2 ENERGY-WEIGHTED SUM RULES

Appendix A is presented in Table A1.

REFERENCES

- Ajzenberg-Selove, F., 1977, Nucl. Phys. A **281**, 1.
- Arkatov, Y. M., T. I. Vatsset, V. I. Volschuk, V. V. Kirichenko, I. M. Prokhorets, and A. F. Khodyachikh, 1971, Sov. J. Nucl. Phys. **12**, 123.
- Arthur, E. D., D. M. Drake, and I. Halpern, 1974, Phys. Rev. Lett. **35**, 914.
- Baldin, A. M., V. I. Goldanskii, and I. L. Rosental, 1961, *Kinematics of Nuclear Reactions* (Oxford U. P., London).
- Barbour, I. M., and J. A. Hendry, 1972, Phys. Lett. B **38**, 151.
- Bergqvist, I., D. M. Drake, and D. R. McDaniels, 1974, Nucl. Phys. A **231**, 29.
- Bergqvist, I., and M. Potokar, 1979, in *Neutron Capture Gamma-Ray Spectroscopy*, edited by Robert Chrien and Walter R. Kane (Plenum, New York), p. 299.
- Bertrand, F. E., 1976, Ann. Rev. Nucl. Sci. **26**, 457.
- Bertsch, G., J. Borysowicz, H. McManus, and W. G. Love, 1977, Nucl. Phys. A **284**, 399, 412.
- Brown, G. E., 1964, Nucl. Phys. **57**, 339.
- Brown, G. E., 1967, *Unified Theory of Nuclear Models* (North-Holland, Amsterdam), 2nd ed.
- Buck, B., and A. A. Pilt, 1977, Nucl. Phys. A **280**, 133.
- Bussoletti, J. E., 1978 Ph. D. thesis, University of Washington.
- Bussoletti, J. E., K. A. Snover, K. Ebisawa, T. A. Trainor, H. E. Swanson, E. G. Adelberger, and R. Helmer, 1976, Bull. Am. Phys. Soc. **21**, 996.
- Calarco, J. R., S. W. Wissink, M. Sasao, K. Wienhard, and S. S. Hanna, 1977, Phys. Rev. Lett. **39**, 925.
- Cameron, C. P., N. R. Roberson, D. G. Rickel, R. D. Ledford, H. R. Weller, R. A. Blue, and D. R. Tilley, 1976, Phys. Rev. C **14**, 553.
- Carr, R. W., and J. E. E. Baglin, 1971, Nucl. Data Tables **10**, 143.
- Clement, C. F., A. M. Lane, and J. A. Rook, 1965, Nucl. Phys. **66**, 273 and 293.
- Collins, M. T., C. C. Chang, S. L. Tabor, G. J. Wagner, and J. R. Wu, 1979, Phys. Rev. Lett. **42**, 1440.
- Cvelbar, C. F., and S. L. Whetstone, 1974, in *Charged-Particle-Induced Radiative Capture*, (International Atomic Energy Agency, Vienna), p. 271.
- Dehesa, J. S., S. Krewald, J. Speth, and A. Faessler, 1977, Phys. Rev. C **15**, 1858.
- DeJager, C. W., L. H. DeVries, and L. C. DeVries, 1974, At. Data and Nucl. Data Tables **14**, 479.
- Devons, S., and L. J. B. Goldfarb, 1957, in *Handbuch der Physik*, edited by S. Flügge, (Springer, Berlin) Vol. **42**, p. 362.
- Dietrich, F. S., D. W. Heikkinen, K. A. Snover, and K. Ebisawa, 1977, Phys. Rev. Lett. **38**, 156.
- Dietrich, F. S., and A. K. Kerman, 1979, Phys. Rev. Lett. **43**, 114.
- Drosg, M., and D. M. Drake, 1974, LA-5732-MS, Los Alamos Scientific Laboratory.
- Endt, P. M., and C. Van der Leun, 1973, Nucl. Phys. A **214**, 1.
- Ferguson, A. J., 1965, *Angular Correlation Methods in Gamma-Ray Spectroscopy*, (North-Holland, Amsterdam).
- Feshbach, H., 1962, Ann. Phys. (NY) **19**, 287.
- Feshbach, H., A. K. Kerman, and R. H. Lemmer, 1967, Ann. Phys. (NY) **41**, 230.
- Foote, G. S., D. Branford, D. C. Weissner, N. Shikazono, R. A. I. Bell, and F. C. P. Huang, 1976, Nucl. Phys. A **263**, 349.
- Foote, G. S., D. Branford, N. Shikazono, and D. C. Weissner, 1974, J. Phys. A (:Math., Nucl. Gen.) **7**, L27.
- Foote, G. S., D. Branford, D. C. Weissner, N. Shikazono, and F. C. P. Huang, 1974, J. Phys. A.: Math., Nucl. Gen. **7**, 14.
- Frederick, D. E., R. J. J. Stewart, and R. C. Morrison, 1969, Phys. Rev. **186**, 992.
- Fukuda, S., and Y. Torizuka, 1972, Phys. Rev. Lett. **29**, 1109.
- Gell-Mann, M., and V. L. Telegdi, 1953, Phys. Rev. **91**, 169.
- Gemmell, D. S., and G. A. Jones, 1962, Nucl. Phys. **33**, 102.
- Gibson, B. F., 1979, Los Alamos Scientific Laboratory, Los Alamos, New Mexico, private communication (unpublished).
- Glavish, H. F., 1973, in "Fifth Symposium on the Structure of Low-Medium Mass Nuclei," edited by J. P. Davidson and Bernard D. Kern, University Press of Kentucky, Lexington, p. 233.
- Glavish, H. F., 1973, in "International Conference on Photonic Nuclear Reactions and Applications" Vol. II, ed. by Barry L. Berman, (U.S.A.E.C. Office of Information Services, Oak Ridge, TN), Vol. II, p. 755.
- Glavish, H. F., 1976, in "Proceedings of the Fourth International Symposium on Polarization Phenomena in Nuclear Reactions," edited by W. Gruebler and V. König., Birkhäuser Verlag, Basel, p. 317.
- Glavish, H. F., S. S. Hanna, R. Avida, R. N. Boyd, C. C. Chang, and E. Diener, 1972, Phys. Rev. Lett. **28**, 766.
- Halderson, Dean, 1978, Nucl. Phys. A **303**, 359.
- Halderson, Dean, and R. J. Philpott, 1979, Phys. Rev. Lett. **42**, 36.
- Hanna, S. S., 1972, in *Nuclear Structure Studies Using Electron Scattering and Photoreaction*, edited by K. Shoda and H. Ui, Supplement to Research Report of Laboratory of Nuclear Science, Tohoku University, Vol. 5, p. 453.
- Hanna, S. S., 1973, in *International Conference on Photonic Nuclear Reactions and Applications*, 1973, edited by Barry L. Berman, (U.S.A.E.C. Office of Information Services, Oak Ridge, TN), Vol. I, p. 417.
- Hanna, S. S., 1974, in *Proceedings of the International Conference on Nuclear Structure and Spectroscopy*, edited by H. P. Blok and A. E. L. Dieperink, (Scholar's Press, Amsterdam), Vol. 1, p. 249.
- Hanna, S. S., 1977, in *Lecture Notes in Physics*, edited by S. Costa and C. Schaerf, (Springer-Verlag, Berlin), Vol. 61, p. 275.
- Hanna, S. S., 1979, in *Proceedings of the International Conference on Nuclear Physics with Electromagnetic Interactions*, edited by H. Arenhövel and D. Drechsel, (Springer-Verlag, Berlin), p. 288.
- Hanna, S. S., H. F. Glavish, R. Avida, J. R. Calarco, E. Kuhlmann, and R. LaCanna, 1974, Phys. Rev. Lett. **32**, 114.
- Hanna, S. S., H. F. Glavish, E. M. Diener, J. R. Calarco, C. C. Chang, R. Avida, and R. N. Boyd, 1972, Phys. Lett. B **40**, 631.
- Harakeh, M. H., P. Paul, H. M. Kuan, and E. K. Warburton, 1975, Phys. Rev. C **12**, 1410.
- Hayward, E., 1970, Natl. Bur. Stand. (U.S.) Monograph. No. 118, Washington, DC.
- Hayward, Evans, William R. Dodge, and Bryan H. Patrick, 1979, Nucl. Instr. and Methods **159**, 289.
- Hauser, W., and H. Feshbach, 1952, Phys. Rev. **87**, 366.
- Jensen, M., D. R. Tilley, H. R. Weller, N. R. Roberson, S. A. Wender, and T. B. Clegg, 1979, Phys. Rev. Lett. **43**, 609.
- Kabachnik, N. M., and V. N. Rayuvaev, 1976, Phys. Lett. B **61**, 420.
- Kerman, A. K., 1980, private communication.
- King, George, III, 1978, Ph. D. thesis, Stanford University, unpublished.
- Knöpfle, K. T., 1979, in *Proceedings of the International Conference on Nuclear Physics with Electromagnetic Interactions*, edited by H. Arenhövel and D. Drechsel, (Springer-

- Verlag, Berlin), p. 311.
- Knöpfle, K. T., G. J. Wagner, H. Brewer, M. Rogge, and C. Mayer-Böricke, 1975, *Phys. Rev. Lett.* **35**, 779.
- Knöpfle, K. T., G. J. Wagner, P. Paul, H. Breuer, C. Mayer-Böricke, M. Rogge, and P. Turek, 1978, *Phys. Lett. B* **74**, 191.
- Kuan, H. M., M. Hasinoff, W. J. O'Connell, and S. S. Hanna, 1970, *Nucl. Phys. A* **151**, 129.
- Kuhlmann, E., J. R. Calarco, V. K. C. Cheng, D. G. Mavis, J. R. Hall, and S. S. Hanna, 1979, *Phys. Rev. C* **20**, 5.
- Kuhlmann, E., E. Ventura, J. R. Calarco, D. G. Mavis, and S. S. Hanna, 1975, *Phys. Rev. C* **11**, 1525.
- La Canna, R., 1977, Ph. D. thesis, Stanford University, unpublished.
- La Canna, R., H. F. Glavish, J. R. Calarco, and S. S. Hanna, 1977, Progress Report, Nuclear Physics Group, Stanford University, pp. 22-26.
- Laszewski, R. M., and R. J. Holt, 1977, *At. Data Nucl. Data Tables* **19**, 305.
- Lees, E. W., A. Johnston, S. W. Brain, C. S. Curran, W. A. Gillespie, and R. P. Singhal, 1974, *J. Phys. A* **7**, 936.
- Lewis, M. B., and F. E. Bertrand, 1972, *Nucl. Phys. A* **196**, 337.
- Likar, A., A. Lindholm, L. Nilsson, I. Bergqvist, and B. Palsson, 1978, *Nucl. Phys. A* **298**, 217.
- Likar, A., M. Potokar, and F. Cvelbar, 1977, *Nucl. Phys. A* **280**, 49, and references therein.
- Lisowski, P. W., R. L. Walter, C. E. Busch, and T. B. Clegg, 1975, *Nucl. Phys. A* **242**, 298.
- Lushnikov, A. A., and D. F. Zaretsky, 1965, *Nucl. Phys.* **66**, 35.
- Marrs, R. E., E. G. Adelberger, K. A. Snover, and M. D. Cooper, 1975, *Phys. Rev. Lett.* **35**, 202.
- Mavis, D. G., 1977, Ph. D. thesis, Stanford University, unpublished.
- Meyerhof, W. E., M. Suffert, and W. Feldman, 1970, *Nucl. Phys. A* **148**, 211.
- Meyer-Schützmeister, L., R. E. Segel, K. Raghunathan, P. T. Debevac, W. R. Wharton, L. L. Rutledge, and T. R. Ophel, 1978, *Phys. Rev. C* **17**, 56.
- Meyer-Schützmeister, L., Z. Vager, R. E. Segel, and P. P. Singh, 1968, *Nucl. Phys. A* **108**, 180.
- Moss, J. M., C. M. Rozsa, J. D. Bronson, and D. H. Youngblood, 1974, *Phys. Lett. B* **53**, 51.
- Nathan, O., and S. R. Nilsson, 1965, in *Alpha-, Beta-, and Gamma-Ray Spectroscopy*, edited by K. Siegbahn, Vol. 2, North-Holland, Amsterdam, p. 1020.
- O'Connell, W. J., and S. S. Hanna, 1978, *Phys. Rev. C* **17**, 892.
- Paul, P., 1974, in *Nuclear Spectroscopy and Reactions, Part A*, edited by Joseph Cerny, (Academic Press, New York), p. 345.
- Paul, P., 1977, in *Elementary Modes of Excitation in Nuclei*, edited by A. Bohr and R. A. Broglia, (North-Holland, Amsterdam), p. 495.
- Peschel, R. E., J. M. Long, H. D. Shay, and D. A. Bromley, 1974, *Nucl. Phys. A* **232**, 269.
- Pitthan, R., and Th. Walcher, 1971, *Phys. Lett. B* **36**, 563.
- Potokar, M., 1973, *Phys. Lett. B* **46**, 346.
- Potokar, M., 1978, private communication.
- Potokar, M., A. Likar, M. Budnar, and F. Cvelbar, 1977, *Nucl. Phys. A* **277**, 29.
- Rolfs, C., 1973, *Nucl. Phys. A* **217**, 29.
- Rolfs, C., 1974, in *Charged-Particle-Induced Radiative Capture*, (International Atomic Energy Agency, Vienna), p. 197.
- Seyler, R. G., and H. R. Weller, 1979, *Phys. Rev. C* **20**, 453.
- Seyler, R. G., and H. R. Weller, 1979, *Atomic Data and Nuclear Data Tables* **23**, 99.
- Singh, P. P., R. E. Segel, L. Meyer-Schützmeister, S. S. Hanna, and R. G. Allas, 1965, *Nucl. Phys.* **65**, 577.
- Skopik, D. M., H. R. Weller, N. R. Roberson, and S. A. Wender, 1979, *Phys. Rev. C* **19**, 601.
- Snover, K. A., 1979, in *Neutron Capture Gamma-Ray Spectroscopy*, edited by Robert E. Chrien and Walter R. Kane (Plenum, New York), p. 319; and private communication.
- Snover, K. A., E. G. Adelberger, and D. R. Brown, 1974, *Phys. Rev. Lett.* **32**, 1061.
- Snover, K. A., J. E. Bussolletti, K. Ebisawa, T. A. Trainor, and A. B. McDonald, 1976, *Phys. Rev. Lett.* **37**, 273.
- Snover, K. A., P. G. Ikossi, and T. A. Trainor, 1979, *Phys. Rev. Lett.* **43**, 117.
- Stewart, R. J. J., R. C. Morrison, and D. E. Frederick, 1969, *Phys. Rev. Lett.* **23**, 323.
- Stroetzel, M., and A. Goldman, 1970, *Z. Phys.* **233**, 245.
- Suffert, M., and W. Feldman, 1967, *Phys. Lett. B* **24**, 579.
- Turner, J. D., C. P. Cameron, N. R. Roberson, H. R. Weller, and D. R. Tilley, 1978, *Phys. Rev. C* **17**, 1853.
- Turner, J. D., N. R. Roberson, S. A. Wender, H. R. Weller, and D. R. Tilley, 1979, *Phys. Rev. C* **21**, 525.
- Watson, R. B., D. Branford, J. L. Black, and W. J. Caelli, 1973, *Nucl. Phys. A* **203**, 209.
- Weller, H. R., N. R. Roberson, D. Rickel, C. P. Cameron, R. D. Ledford, and T. B. Clegg, 1974, *Phys. Rev. Lett.* **32**, 177.
- Weller, H. R., R. A. Blue, N. R. Roberson, D. G. Rickel, S. Maripuu, C. P. Cameron, R. D. Ledford, and D. R. Tilley, 1976, *Phys. Rev. C* **13**, 922.
- Weller, H. R., N. R. Roberson, and S. R. Cotanch, 1978, *Phys. Rev. C* **18**, 65.
- Welton, T. A., 1963, in *Fast Neutron Physics*, edited by J. B. Marion and J. L. Fowler (Interscience, New York), Vol. II, p. 1317.
- Wender, S. A., N. R. Roberson, M. Potokar, H. R. Weller, and D. R. Tilley, 1978, *Phys. Rev. Lett.* **41**, 1217.
- Wender, S. A., N. R. Roberson, D. R. Tilley, and H. R. Weller, 1980, to be published.
- Yamagata, T., K. Iwamoto, S. Kishimoto, B. Saeki, K. Yuasa, M. Tanaka, T. Fukuda, K. Kokado, I. Miura, M. Inove, and H. Ogata, 1978, *Phys. Rev. Lett.* **40**, 1028.
- Youngblood, D. H., A. D. Bacher, D. R. Brown, J. D. Bronson, J. M. Moss, and C. M. Rozsa, 1977, *Phys. Rev. C* **15**, 246.
- Youngblood, D. H., J. M. Moss, C. M. Rozsa, J. D. Bronson, A. D. Bacher, and D. R. Brown, 1976, *Phys. Rev. C* **13**, 994.